

Toward Visualizing Genomic DNA Using Electron Microscopy via DNA Metallization

Xuelin Jin, Shrute Kannappan, Natalia Diyah Hapsari, Yu Jin, Kyeong Kyu Kim,*
Jung Heon Lee,* and Kyubong Jo*

Electron microscopy-based DNA imaging is a powerful tool that provides a high resolution for observing genomic structures involved in biochemical processes. The first method, heavy metal shadow casting, was developed in 1948. Uranyl acetate has been widely used for DNA electron microscopic imaging since the 1960s. However, for this method, scientists must deal with government regulations for the safety and disposal. Additionally, sample preparation is often complicated and time-consuming. Recently, nanoparticles and nanowires have emerged as a new way of imaging DNA molecules under both transmission and scanning electron microscopes. However, as this technology is still in its early stages, there is room for further development. In this review, heavy metal staining, nanoparticle staining, and nanowire growth for DNA visualization are introduced. The applications of shadow casting and uranyl acetate staining in the visualization of DNA structures and protein–DNA complexes are discussed. Then, nanomaterial-based DNA staining methods are covered, including electrostatic interactions, DNA chain modification, reducing-group-modified DNA ligands and DNA–peptide/protein interactions. This review provides up-to-date information on different DNA staining approaches and their applications in DNA studies. Ultimately, it offers a new direction for genome analysis through DNA visualization.

1. Introduction

DNA encodes the genetic information that is used to build and maintain all living organisms. This information can be decoded using DNA sequencing technologies. The rapid development of DNA sequencing has revolutionized the field of genetics and related biomedical sciences and engineering. In 1980, Sanger and Gilbert received the Nobel Prize for their development of DNA sequencing.^[1] Newer and faster methods for DNA sequencing, such as next-generation sequencing (NGS), emerged,^[2] making it possible to sequence entire genomes. Recently, single-molecule-based long-read sequencing technologies emerged,^[3] allowing scientists to read the telomere-to-telomere sequence of the human genome.^[4] In January 2023, Nature Methods named “long-read sequencing” as the Method of the Year 2022.^[5] Despite advancements in sequencing technologies, they have limitations.^[6] The ultimate goal of genomic DNA analysis is to not only determine the sequence, but

X. Jin
College of Agriculture
Yanbian University
977 Gongyuan Street, Yanji City, Jilin Province 133000, P. R. China


S. Kannappan, K. K. Kim
Department of Precision Medicine
School of Medicine
Sungkyunkwan University
2066 Seobu-Ro, Jangan-Gu, Suwon-Si, Gyeonggi-Do 16419, Republic of Korea
E-mail: kyeongkyu@skku.edu

S. Kannappan, J. H. Lee
Research Center for Advanced Materials Technology
Core Research Institute
2066 Seobu-Ro, Jangan-Gu, Suwon-Si, Gyeonggi-Do 16419, Republic of Korea
E-mail: jhlee7@skku.edu

N. D. Hapsari
Chemistry Education Program
Department of Mathematics and Science Education
Sanata Dharma University
29 Tasura Street, Maguwoharjo, Depok, Krodan, Maguwoharjo, Sleman, Yogyakarta 55281, Indonesia

Y. Jin, K. Jo
Department of Chemistry
Sogang University
35 Baekbeom-ro, Mapo-gu, Seoul 04107, Republic of Korea
E-mail: jokyubong@sogang.ac.kr

J. H. Lee
School of Advanced Materials Science and Engineering
Sungkyunkwan University
2066 Seobu-Ro, Jangan-Gu, Suwon-Si, Gyeonggi-Do 16419, Republic of Korea

 The ORCID identification number(s) for the author(s) of this article can be found under <https://doi.org/10.1002/ssr.202200361>.

© 2023 The Authors. Small Structures published by Wiley-VCH GmbH. This is an open access article under the terms of the Creative Commons Attribution License, which permits use, distribution and reproduction in any medium, provided the original work is properly cited.

DOI: 10.1002/ssr.202200361

also capture the natural conformational, epigenetic information, and protein–DNA interactions without the need for fragmentation, amplification, or the introduction of functional moieties.

Given these concerns, electron microscopy (EM) offers a powerful and promising solution for obtaining high-resolution images of DNA molecules. Unlike optical microscopy, which is limited by the diffraction of light,^[7] EM is capable of capturing images of smaller molecular structures and providing detailed information about DNA structure and its complex. The power of DNA imaging can be further increased when combined with sequencing technology, allowing for the simultaneous visualization and analysis of large DNA molecules with high precision and accuracy. In addition, EM is also useful for visualizing a variety of biochemical reactions on large DNA molecules, including DNA damage and protein–DNA interactions. This makes it an important tool for understanding the complex processes that occur within cells and for developing new therapies for a range of diseases. Overall, the use of EM for DNA visualization and analysis represents an important direction for the development of advanced nanoscience and technology and has the potential to transform our understanding of the biological world.

Since the first DNA visualization by Scott in 1948,^[8] transmission electron microscopy (TEM) has been used to visualize DNA,^[9] chromatin,^[10] and protein–DNA complexes.^[11] However, obtaining clear images using EM is challenging because DNA is thin and composed of light elements (H, N, C, O, P) that have low electron scattering properties. As a solution, uranyl acetate has been used to enhance the contrast of DNA images by binding to the DNA phosphate backbone through electrostatic interactions, due to its electron-rich properties.^[12,13] However, unlike in the 1960s, uranium is no longer practical in biochemistry laboratories due to the requirement for government permission to access it. An alternative to uranyl acetate is the metallization of DNA using nanoparticles or nanowires. The deposited metal acts as a strong contrast agent and increases the diameter of the metalized DNA, making it easier to visualize using a scanning electron microscope (SEM). SEM can be a preferred tool for genomic DNA analysis due to its accessibility, ease of sample preparation, and the ability to cover millimeter-scale areas. Therefore, DNA metallization can be a solution for visualizing DNA molecules. However, to date, DNA metallization using nanoparticle stain or nanowire growth has primarily been focused on the development of nanostructures and has not received much attention for genomic DNA analysis.

In this article, we review the current DNA metallization technologies that can be applied to genomic DNA imaging and analysis. We first examine the traditional uranyl acetate staining method and how it has been used to visualize genomic DNA in various studies, such as various DNA structures, DNA–protein interactions, and chromatin structures using EM. Then, we introduce DNA metallization through nanoparticles and nanowires and explore their potential for genomic DNA visualization. This review serves as a foundation for the development of a next-generation platform for visualizing genomic DNA under EM.

2. Visualizing Genomic DNA through Heavy Metal Staining

2.1. DNA Structures under EM

EM enables high-resolution observation of DNA features such as size, structure, and base distribution, as well as protein–DNA interactions, with a level of detail as small as 50–100 nucleotides. In the early years of EM-based DNA imaging (1948), the “shadow cast” method was used, in which heavy metal was deposited onto the DNA specimen at an oblique angle.^[8,14] This resulted in metal deposition on surfaces facing the source and created a shadow for direct DNA visualization, as shown in **Figure 1A**.^[8,15] **Figure 1B** shows genomic DNA of T2 bacteriophage through the shadow casting approach.^[16] Soon after, heavy metal salts such as uranyl acetate were used to stain the DNA with the shadow-casting method, resulting in enhanced contrast during EM observation.^[12,17] Uranyl acetate allows for the staining of DNA molecules adsorbed to carbon films^[18–20] or cytochrome spread DNA during dark field visualization.^[21] Uranyl formate is also capable of staining DNA molecules and DNA–protein complexes.^[20] However, it is unstable and must be used immediately after preparation.

Uranyl acetate-based staining combined with platinum shadow casting has been the most popular method for EM-based genome analysis. The local base composition, orientation, and intramolecular base heterogeneity of DNA can be determined by exploiting the difference in thermostability between A/T-rich and G/C-rich regions through the “partial denaturation map” as shown in **Figure 1C**.^[13,22] Various hybridization techniques have been used to study DNA–DNA interactions (D-loops, heteroduplex junctions),^[23] DNA–RNA interactions (R-loops),^[13] and DNA–protein interactions (RNA polymerase localization).^[19] Another method involves using terminal deoxynucleotidyl transferase (TdT) in combination with a radioisotope-labeled dATP for EM autoradiography-based DNA localization.^[24] Notable applications of these EM-based methods in genome analysis include the identification of RNA splicing mechanisms in eukaryotes through R-loop formation,^[25] the characterization of eukaryotic DNA replication forks,^[26] the determination of nucleosome hierarchy,^[27] DNA repair pathways,^[28] the determination of DNA length,^[29] replication fork reversal and its role in fork degradation,^[30] DNA supercoiling and knotting,^[31] and the localization of replication foci during different points in the S-phase of DNA replication.^[32]

EM allows observation of replication forks as shown in **Figure 1D**, gDNA aggregation with protein clusters, and nonspecific four-way DNA structures.^[33] EM has also been used to study the chronological effects of DNA damage agents, such as genotoxic agents,^[34] UV radiation,^[35] and replication fork reversal.^[36] Additionally, the hierarchical branching of chromatin structure at the nanoscale has been visualized through uranyl acetate-based staining.^[37] DNA EM also provides the capability to visualize DNA topology in chromatin with differing nucleosome spacing, which results in distinct higher order structures with either active or repressed genes.^[38] **Figure 1E** depicts a replication fork, including two daughter strands, a single parental strand, ssDNA gaps on the daughter strands, and ssDNA gap at the replication fork junction.^[39] EM has both advantages

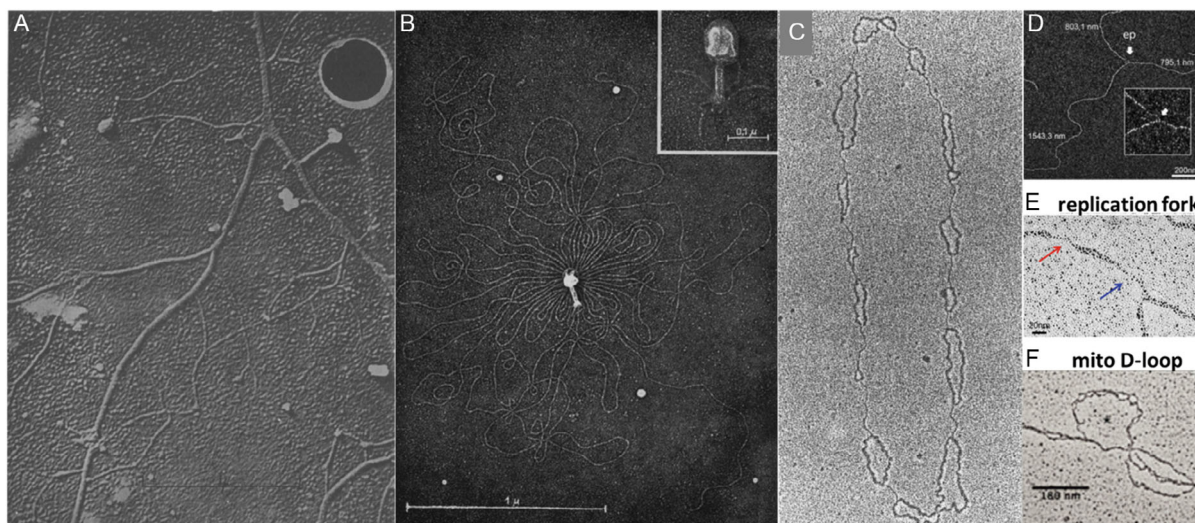


Figure 1. Electron microscopic DNA images. A) The first EM image of DNA in 1948. Reproduced with permission.^[8] Copyright 1948, Elsevier. B) Genomic DNA of T2 bacteriophage via shadow casting. Reproduced with permission.^[16] Copyright 1962, Elsevier. C) DNA partial denaturation mapping by uranyl acetate and Pt shadowing. Reproduced with permission.^[13] Copyright 1981, Taylor & Francis. D) DNA replication fork stained by Pt shadow casting. Reproduced with permission.^[33] Copyright 2020, Oxford University Press. E) Replication fork and single-stranded DNA gaps at junction sites. Reproduced with permission.^[39] Copyright 2022, Springer. F) Mitochondrial D-loops and some single-stranded DNA denaturation bubbles via uranyl acetate and Pt shadowing. Reproduced with permission.^[41] Copyright 2021, Oxford University Press.

and disadvantages for the observation of DNA replication forks.^[40] On one hand, DNA EM of replication forks provides clear images with a high resolution of 40 nucleotides and actual visualization of ssDNA gaps, both on the daughter strands and at replication forks, thereby allowing for the analysis of the positions and numbers of ssDNA gaps at replication forks. However, for detection, the ssDNA gaps must be near the replication forks and longer than 40 nucleotides.

In addition to the study of genomic DNA, EM has also been used to characterize the mitochondrial DNA replication cycle, as shown in Figure 1F.^[41] Furthermore, DNA EM allows for visualization of various structures such as plasmid DNA, ss–ds DNA, ssDNA gap between dsDNA, holiday junction of DNA, D-loop, strand exchanges, and DNA intermediates formed during DNA damage repair.^[33,42]

2.2. DNA–Protein Interaction under EM

Many studies have utilized uranyl acetate staining in DNA EM to reveal DNA–protein interactions. **Figure 2A** shows the transcription of rDNA genes by RNA polymerase I and III.^[43] The incorporation of the locus-foreign gene HSX1 and the locus-native gene RDN5 resulted in an enrichment of RNA polymerase III complexes. This method can detect the insertion of gene clusters and directly visualize the gene clusters.

While uranyl acetate has been the most common dye used for staining DNA, the development of alternative safe and nonradioactive is quintessential due to its biological toxicity and radioactivity. As alternative contrast agents, the lanthanum salts,^[44] osmium tetroxide,^[45] hafnium chloride,^[46] phosphotungstic acid,^[47] Pt-blue,^[48] and oolong tea^[49] have been developed for the EM visualization of DNA molecules. For example, Miller

et al. visualized the Miller tree with phosphotungstic acid staining of EM in 1969, as shown in Figure 2B.^[50]

2.3. Chromatin Structure under EM

The EM has a much higher resolution and can capture images of smaller molecular structures that cannot be seen using a light microscope, which is limited by the diffraction of light. This high-resolution imaging capability makes EM an invaluable tool for studying the 3D dynamics of chromatin structure and other cellular components. However, EM imaging also has some limitations, such as the difficulty in obtaining structural information about live cells or tissues, and the lack of specificity in labeling certain molecules or structures of interest. To overcome these limitations, correlative light and electron microscopy (CLEM) has been developed as a hybrid technique that combines the advantages of both light and EM. CLEM allows researchers to first image the sample using light microscopy, which enables the visualization of specific molecules or structures of interest using fluorescent probes or antibodies. The same sample is then imaged using EM, which provides high-resolution structural information about the same molecules or structures. By combining these two imaging modalities, it is possible to obtain detailed information about the structure and function of complex biological systems with high accuracy and resolution. CLEM has become an important tool for studying the 3D dynamics of chromatin structure, as well as other biological processes that involve complex molecular interactions and structures.^[51]

Another innovative strategy for visualizing DNA involves the use of DNA-binding fluorescent small molecules. These molecules can be designed to selectively bind to DNA and emit fluorescence upon excitation with light of a certain wavelength.

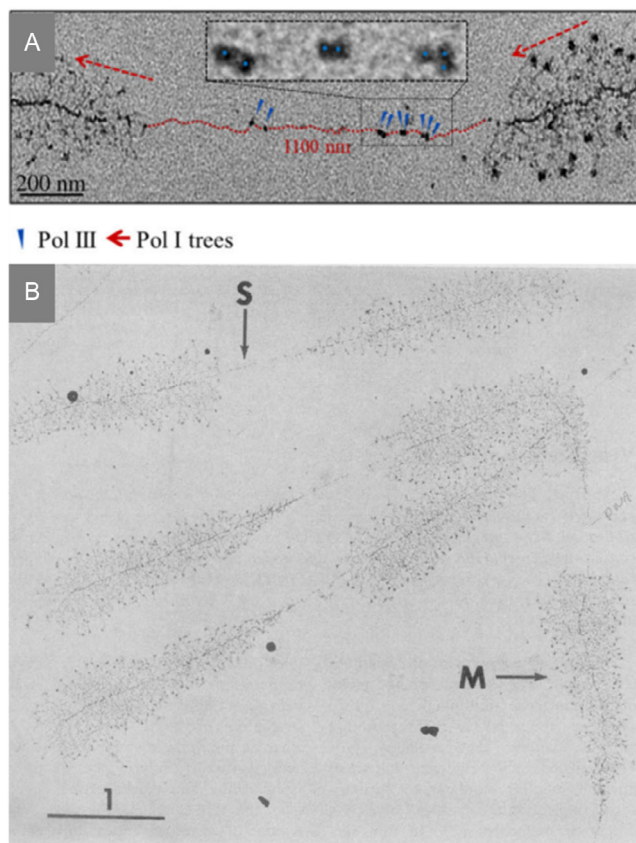


Figure 2. DNA–protein complexes under EM. A) Miller trees of clone showing RNA polymerase III complexes and RNA polymerase I. Reproduced with permission.^[43] Copyright 2021, Springer Nature. B) Miller tree by Miller et al. in 1969. Nucleolar cores isolated from *Triturus viridescens* oocyte showed matrix units (M) and matrix-free segments (s) separating matrix units. Reproduced with permission.^[50] Copyright 1969, AAAS.

By combining these molecules with diaminobenzidine (DAB), a chemical that can undergo local autopolymerization in the presence of hydrogen peroxide, it is possible to induce the formation of precipitates that can be visualized by EM upon staining with osmium tetroxide (OsO_4). One such molecule is DRAQ5, a deep-red fluorescing anthraquinone that has been exploited for CLEM of chromatin organization (ChromEM).^[52] As traditional EM is restricted to 2D space, this method has been combined with EMT to reconstruct the 3D (ChromEMT)^[52] and 4D (nano-ChIA)^[53] chromatin organization down to the ultrastructural level of a single nucleosome as shown in **Figure 3A,B**, respectively. These imaging studies provided the first evidence that the DNA and nucleosomes assemble into disordered chains, with diameters varying between 5 and 24 nm, which are packed at variable densities within the nucleus.^[53] In an attempt to visualize only telomeric regions of the DNA, Hubner et al. developed a genetically modified cell in which the Telomeric repeat-binding factors (TRF1, TRF2) were with eGFP and the peroxidase APEX2.^[54] In these constructs, the eGFP was used for LM imaging of specifically only the telomeres while the APEX2 generated an electron-dense stain for EM upon osmium treatment. Using this technique, the telomeres could be visualized down to the

resolution of ≈ 5 nm, providing the first evidence of the possible direct contact between telomeres and other heterochromatin regions.^[54]

3. DNA Metallization via Metal NP Staining and Nanowire Growth

Metal nanoparticle staining and nanowire growth are two other methods that have been adapted for DNA metallization. In 1998, Braun et al. reported DNA-templated Ag nanowires.^[55] After this pioneering study, DNA-templated metal nanowires have been produced using a variety of metals, including Ag,^[56,57] Au,^[58,59] Cd,^[60,61] Co,^[62] Cu,^[63] Fe,^[64] Ni,^[65] Pd,^[66,67] Pt,^[68,69] Rh,^[70] Te,^[71] Ti,^[72] and MoGe alloys.^[73] DNA nanotechnology has advanced the fabrication of various DNA nanostructures, which allows metal nanostructures to have sophisticated 2D and 3D geometries.^[74] Bottom-up assembly using DNA templates is employed to achieve flexible preparatory platforms for shape-controlled nanofabrication at the molecular and atomic levels.^[75] DNA origami, for example, enabled the self-assembly of specific shapes of DNA structures for the nanofabrication of templates, followed by the metallization of DNA templates.^[76] DNA metallization provides better imaging resolution through EM observation compared to fluorescence microscopies,^[77] and it is an easy, fast, and simple way to fabricate DNA-templated nanostructures with both monometallic and bimetallic compositions.^[78,79] DNA-templated nanostructures via metallization have been intensively studied due to these advantages.

To fabricate DNA-templated nanowires, metal deposition on DNA molecules is important. First, metallic nanoparticles and ions can bind to DNA through electrostatic interactions.^[80,81] Once metal ions bind to DNA templates, they can be reduced for nanowire growth on DNA templates in several ways: chemical reduction,^[82] electrochemical reductions,^[64,83] photoreductions,^[84] reductions by heating,^[85] and other methods.^[60,86] Second, DNA bases chemically modified with reducing groups, such as aldehydes^[87] and sugars,^[78,88] can also be used to reduce metal ions for the deposition of metal nanoparticles on DNA templates, which, in turn, serve as seeds for further nanowire growth.^[78] Third, DNA intercalators with reducing groups can be inserted between DNA base pairs, allowing the reduction of metal ions for the deposition of metal nanoparticles on DNA molecules followed by further DNA metallization.^[89] Fourth, anchors utilizing DNA–peptide/protein interactions can also be exploited for the fabrication of DNA-templated metal nanostructures.^[90] These methods have been widely used for DNA metallization.

In this section, we cover DNA metallization using both metal nanoparticle staining and nanowire growth methods, and later discuss how this can be used for genomic DNA visualization. A review summarizing these procedures for DNA metallization can provide relevant knowledge that can be used in different fields involving the utilization of DNA-templated materials.^[91]

3.1. DNA Metallization through Electrostatic Interaction and Reduction

Figure 4A demonstrates the basic principle of electrostatic interaction between positively charged metal nanoparticles and ions and negatively charged DNA backbones and the following

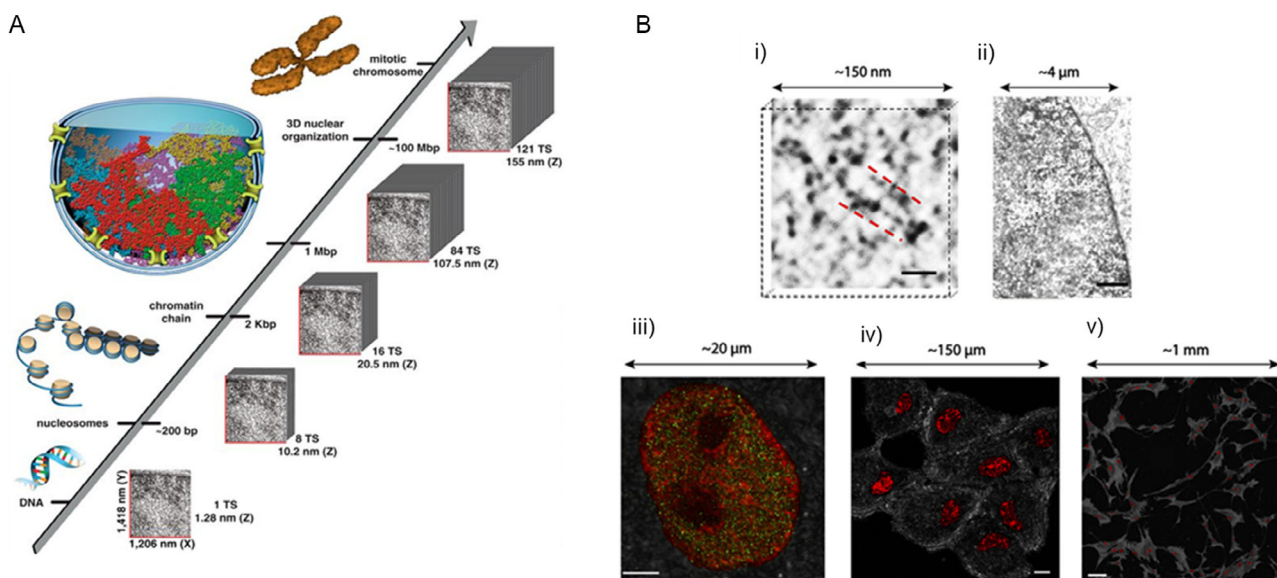


Figure 3. Chromatin hierarchy using EM. A) Schematic of Chrom-EMT used to study 3D chromatin organization. Reproduced with permission.^[52] Copyright 2017, AAAS. B) Representative image of Nano-ChIA capable of capturing different length scales ranging from nm to mm. Reproduced with permission.^[53] Copyright 2021, AAAS.

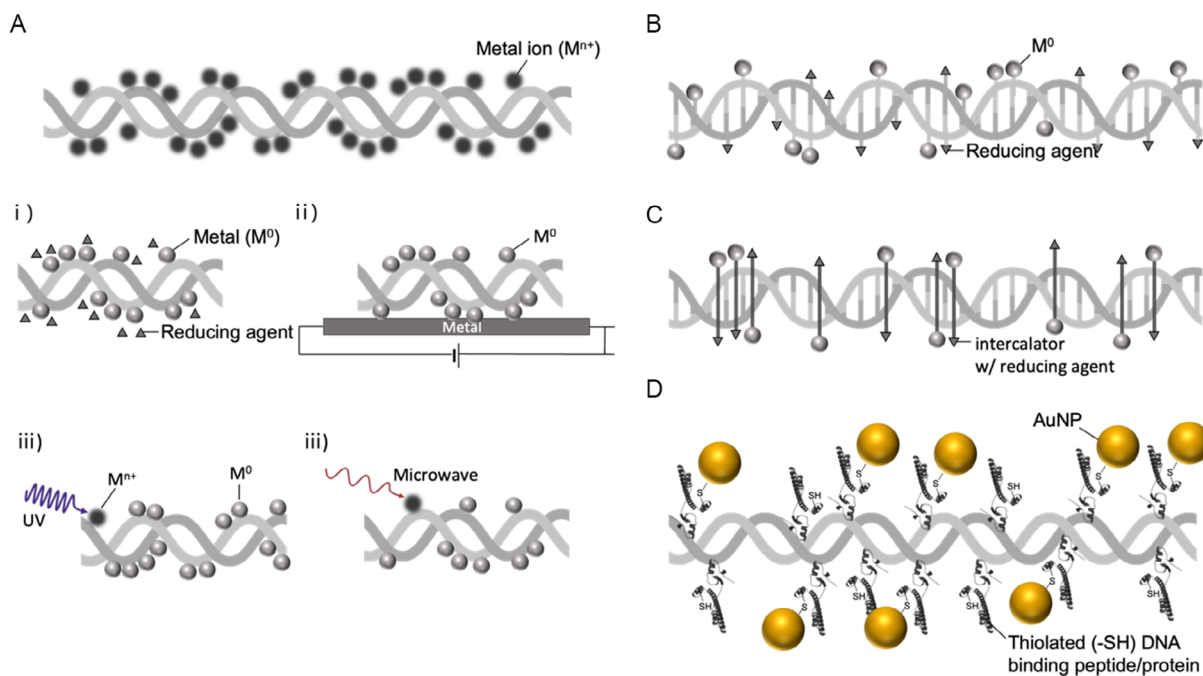


Figure 4. Schematic of DNA metallization using metal NP staining and nanowire growth methods. A) Four approaches using electrostatic interaction. i) chemical reduction with reducing agents, ii) electrochemical reduction on the electrode surface, iii) photoreduction with a light source, and iv) reduction by microwave heating. B) DNA template modification with reducing groups can reduce metal ions to deposit metal on DNA templates. C) Reducing-group-modified DNA intercalators that can reduce metal ions on DNA templates. D) DNA-peptide/protein interaction enables metal NP deposition on DNA templates.

reduction methods: 1) chemical reduction, 2) electrochemical reduction, 3) photoreduction, and 4) reduction by microwave heating. Positively charged metal ions can bind extensively to polyanionic DNA templates through simple electrostatic interactions. Many studies have utilized electrostatic interactions for

the deposition of metal ions on DNA templates, followed by the reduction of the deposited metal ions.

Braun et al. first proposed the principle of DNA metallization using electrostatic interactions and its subsequent reduction, as shown in Figure 6.^[55] They placed λ DNA between two gold

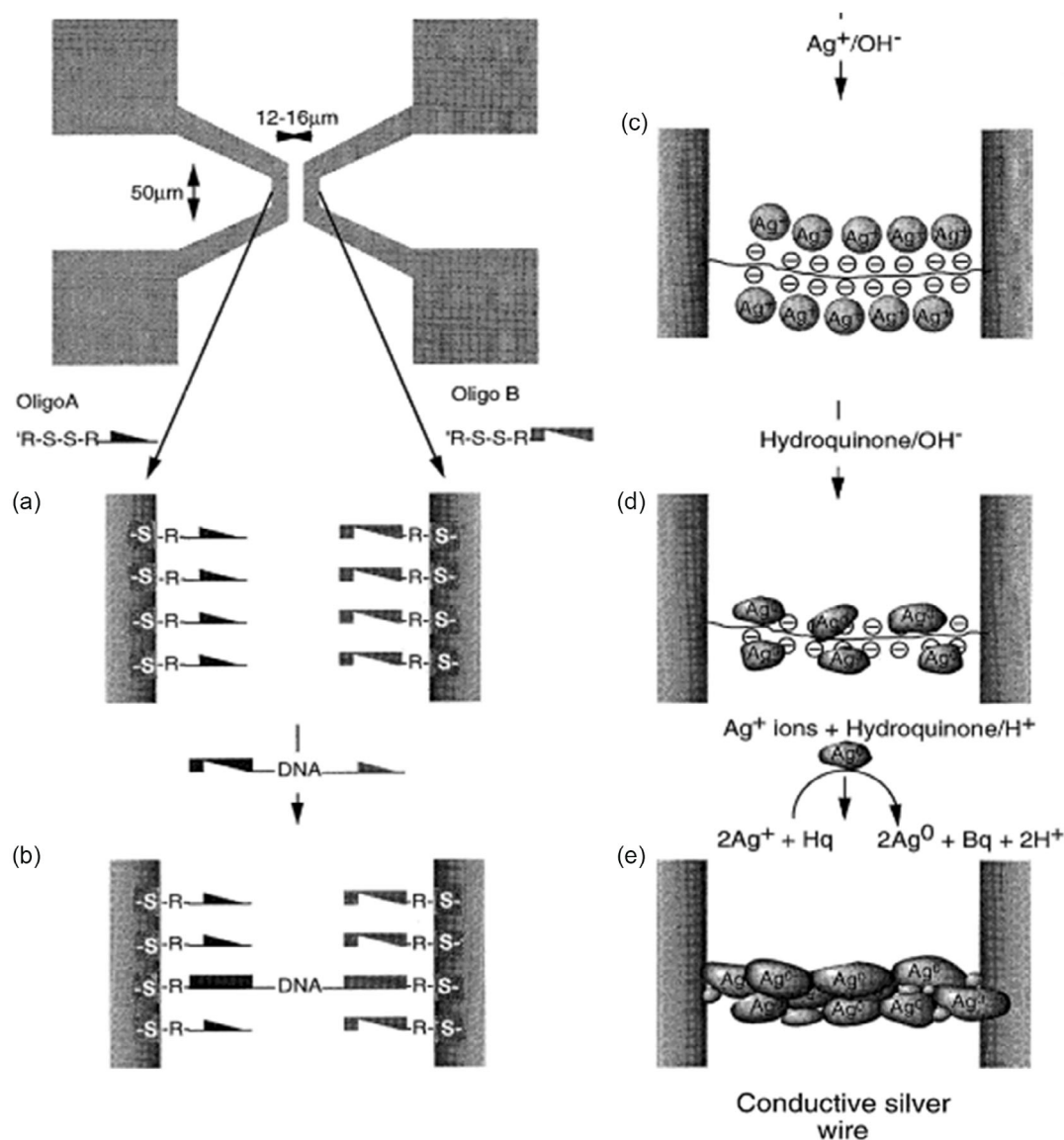


Figure 5. DNA-templated silver nanowire. The top left image is the electrode pattern used for silver nanowire assembly. A) Thiolated oligonucleotides complementary to the sticky ends of λ DNA are attached to the electrodes. B) λ DNA bridge connects the two gold electrodes. C) Silver ions are loaded on the DNA bridge. D) A silver nanowire is assembled by chemical reduction. E) Metallic silver aggregates on the λ DNA. Reproduced with permission.^[55] Copyright 1998, Macmillan.

electrodes (Figure 5A,B), and then bound Ag^+ ions to the λ DNA by replacing Na^+ . This formed Ag–DNA complexes (Figure 5C), which were subsequently reduced by hydroquinone, (Figure 5D), followed by growth (Figure 5E). This procedure generated a conductive DNA-templated Ag nanowire between the gold electrodes. The formation of DNA-templated Ag nanowires was validated by measuring the electrical current between the two gold electrodes. This study inspired the fabrication of DNA-templated metal nanowires with other metal ions such as Au^{3+} ,^[80] Cu^{2+} ,^[92] Ni^{2+} ,^[93] and Pd^{2+} .^[67] In summary, electrostatic interaction has been widely used in DNA metallization, and its application has been extended to the fabrication of various metal nanostructures. The basic principle of DNA metallization

through electrostatic interaction and its subsequent reduction is illustrated in Figure 4A and 5.

3.1.1. Chemical Reduction

In DNA metallization through chemical reduction, the electrostatic interaction between positively charged metal ions and negatively charged DNA backbones produces reactive metal sites that trigger metal nucleation. The reduction process involves the transformation of the reactive metal sites formed in the first step into metal clusters bound to DNA strands. The reduction of metal ions can be achieved using reducing agents such as sodium borohydride, ascorbic acid, dimethylamine borane,

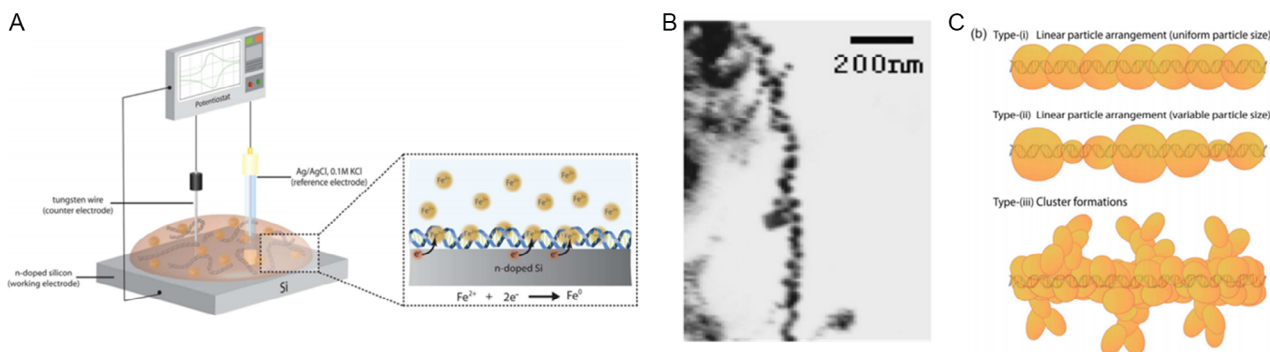


Figure 6. DNA-templated nanowires assembled by electrochemical deposition. A) λ DNA solution containing Fe^{2+} ions loaded on the n-doped Si wafer. The trimethyl silane-modified Si wafer was a working electrode for the electrochemical reduction of Fe ions. The DNA acted as a template for the anisotropic growth of Fe. Reproduced with permission.^[64] Copyright 2013, RSC B) TEM image of DNA-templated Ag nanowires. Reproduced with permission.^[57] Copyright 2007, Elsevier C) Illustrations of type I, the current DNA-templated nanowires (uniform particle size), type II, and type III DNA-templated nanowires prepared by previous methods (various particle sizes and irregular clusters).

and hydroquinone. Figure 5 illustrates the general procedure for chemical reduction, which involves three main steps.^[91]

The first step is the electrostatic interaction, as shown in Figure 5C. The second step is reduction, as shown in Figure 5D. The final step is metal nanowire growth, as shown in Figure 5E. Metal ions can be reduced by reducing agents such as sodium borohydride,^[94] ascorbic acid,^[92] dimethylamine borane,^[62] and hydroquinone.^[95] An excess of reducing agent reduces newly introduced metal ions, unbound metal ions, or metal complexes for further deposition on the metal clusters bound to DNA templates, allowing them to grow into DNA-templated metal nanowires via an autocatalytic process. The metal clusters on the DNA templates play an important role as nucleation sites and catalytic surfaces during the nanowire synthesis process.

The physicochemical properties of DNA-templated metal nanowires depend on various reaction parameters, including metal ion deposition/growth times, concentrations, reactivities of reducing agents, metal ions/DNA ratios, DNA length, DNA sequence, and DNA conformation.^[91] The metals used in the final growth are not necessarily the same as the seeding metals.^[62,79,87] For example, Ni and Cu nanowires on DNA templates can be synthesized by the electrodeless plating of Ni and Cu on Ag-seeded DNA molecules.^[71] These wires can be replaced by Te or Bi_2Te_3 via a galvanic displacement reaction using an acidic solution containing HTeO^{2+} and Bi^{3+} ions.^[71]

There are several strategies for depositing metals on DNA templates by chemical reduction method. The first simple method involves mixing metal ions and DNA in a solution, resulting in the formation of metal–DNA complexes. For example, simple incubation of Na_2PdCl_4 with DNA solution overnight can form a Pd(II)–DNA complex.^[62] The second method is to mix metal-containing compounds with DNA in the presence of sodium citrate, dimethylamine borane, or NaBH_4 . A mixture of K_2PdCl_4 and DNA templates in sodium citrate solution can allow the deposition of metal on the DNA templates.^[96] The third method involves reducing metal-containing compounds with reducing agents to form metal NPs followed by deposition on DNA templates.^[97] For example, HAuCl_4 can be reduced by tris(2-carboxyethyl)phosphine (TCEP) and NaBH_4 to form gold NPs (AuNPs) that seed on DNA templates under acidic conditions for further growth.^[98]

The fourth method is to use metal salts such as AgNO_3 , which directly release metal ions to form metal ion–DNA complexes by simple mixing with DNA solution.^[82] The chemically reduced metal–DNA complex can be formed in both aqueous and organic solutions. For example, DNA and NH_4ReO_4 in an aqueous solution with NaBH_4 generate Re NP deposited DNA templates.^[99] Alternatively, DNA and NH_4ReO_4 in acetonitrile with tetraoctylammonium bromide followed by reduction with NaBH_4 generated metalized DNA template.^[100] Compared to an aqueous solution, an organic solution can prevent the aggregation of metal NPs and generate metal–DNA complexes with monodisperse sizes.^[101]

One way to enhance the power and specificity of DNA metallization is to introduce sequence selectivity. Different DNA bases have varying affinities for different metal ions, and by exploiting these differences, it is possible to selectively deposit metals onto specific DNA sequences. This can be accomplished using DNA–metal adducts, which can help form nanowires on specific DNA sequences.^[68,102] In addition, DNA origamis with specific affinities to their recognition sites can allow site-specific binding of metals on DNA templates, offering a powerful tool for designing nanoscale devices with highly specific properties.^[103] Moreover, selective dsDNA templates also enable the formation of sequence-specific DNA metallization, providing a platform for the development of novel biosensors, nanoelectronic devices, and other materials with tailored properties. Through the combination of selective metallization with DNA origami and other advanced techniques, it is possible to achieve precise control over the formation of complex nanostructures.^[104]

Although the aforementioned method of electrostatic interactions for metal nanowire formation is convenient and widely applied, it still has some disadvantages.^[91] First, the initial deposition step involves electrostatic interactions between positively charged metal ions and negatively charged DNA phosphate backbones, which presents a limitation in the case of nonspecific electrostatic interactions resulting in nonspecific DNA metallization without selectivity and background metal growth. Second, the growth of DNA-templated metal nanowires is rapid, which often results in the formation of irregular and coarse structures. Third, reducing agents may cause the denaturation, contamination, or destruction of the DNA molecules via chemical attack. The issue of the chemical attack

by reducing agents can be avoided by using the following methods such as electrochemical reduction, photoreduction, and reduction by heating because they do not require reducing agents.

3.1.2. Electrochemical Reduction

The electrochemical reduction of metal ions on DNA templates also utilizes electrostatic interactions; however, the metal reduction is performed at the electrode surface rather than by chemical reducing agents. Various metals, such as Ag,^[57,95,105] Rh,^[70] Fe,^[64] and Mn,^[83] have been used for DNA-templated nanowire growth, followed by the reduction and growth of metals bound to DNA strands via electrochemical reduction. Electrochemical reduction possesses two advantages:^[91] the electrochemical process can be performed under ambient conditions without the use of reducing agents, and the electron-transfer rate can be controlled by the potential applied for electrochemical reduction, thereby controlling metal growth.^[106]

In 2007, Cui et al. first used silver for DNA-templated nanowire growth using an electrochemical method as shown in Figure 6B.^[57] DNA templates adsorbed on the electrodes were immersed in a silver ion solution for activation. This was followed by bulk electrolysis via coulometry by applying a potential of 0.3 V

for 3 min to reduce the silver ions. Subsequently, Watson, et al. developed conductive and superparamagnetic DNA-templated Fe nanowires by using DNA and an iron ion solution on n-doped Si <100> wafers, which acted as the working electrodes and substrate for DNA fixation, as shown in Figure 7.^[64] In this method, the deposition of iron ions on the DNA templates facilitated further Fe nucleation, followed by electrochemical reduction of iron ions on the DNA templates fixed on the working electrodes. A simple apparatus can be utilized, and the reaction parameters can be optimized to fabricate fine DNA-templated metal nanowires, as shown in Figure 6C. Another study compared DNA-templated Rh nanowires synthesized by chemical reduction to those prepared by electrochemical reduction.^[70] Compared with chemical reduction, the electrochemical reduction was less efficient because there were still many bare DNA molecules after electrochemical reduction. Moreover, the electrochemical approach is limited to modifying surface-based template structures and poses challenges to sequence-specific DNA metallization.^[91]

3.1.3. Photoreduction

Photoreduction is a fast, clean, and simple method for metal ion reduction. In general, photosensitizers, typically organic ligands,

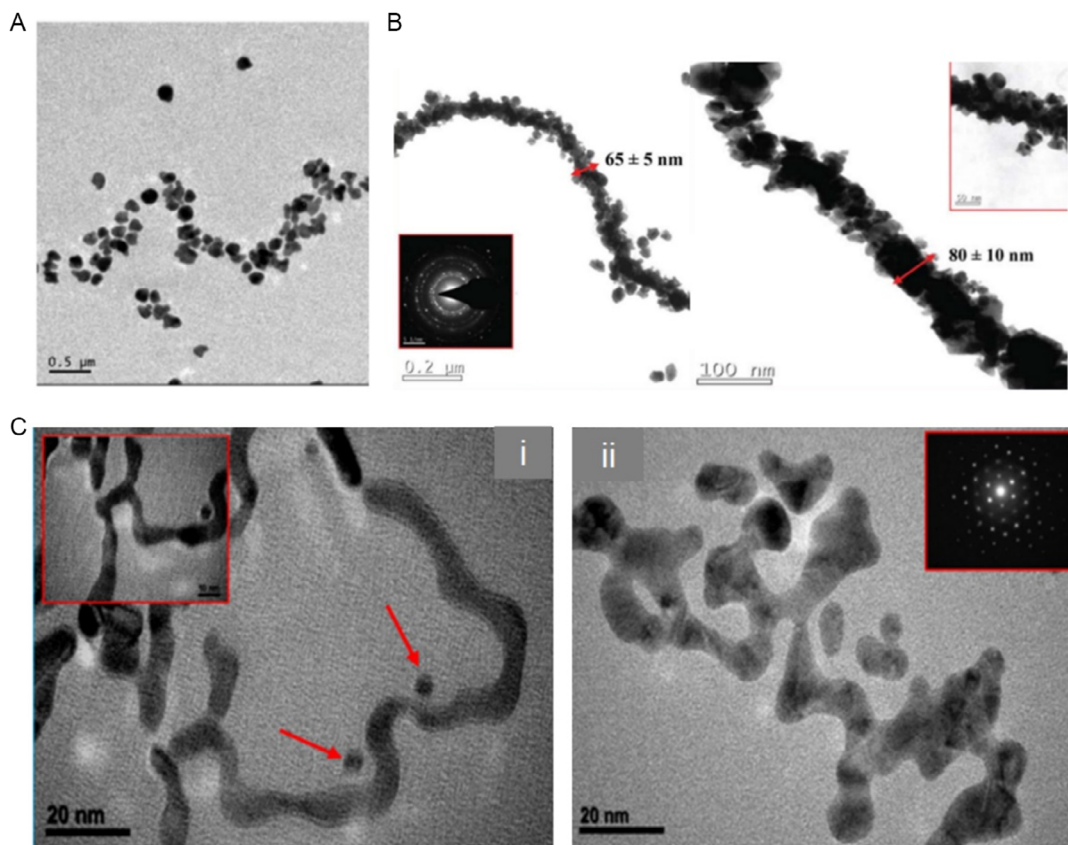


Figure 7. DNA-templated nanowires assembled by UV irradiation. A) TEM micrograph of DNA-templated Au nanoclusters. Reproduced with permission.^[111] Copyright 2008, ACS. B) TEM images of the DNA-templated Au nanowires by photoreduction. Reproduced with permission.^[115] Copyright 2013, RSC C) TEM images of DNA templated Au–Ag nanowires. i) 135 min of UV photoreduction resulted in DNA-templated Au–Ag nanowires with diameters of 2–8 nm. ii) 180 min of UV photoreduction lead to DNA-templated Au–Ag nanowires with diameters of 3–12 nm. Reproduced with permission.^[114] Copyright 2010, Elsevier.

act as both stabilizing agents and catalysts to facilitate metallization.^[107] Because of their intrinsic UV adsorption, DNA molecules can also act as a photosensitizer and a capping ligand for photoinduced metal deposition. In 2005, Berti et al. first used the photoreduction of silver ions attached to DNA templates to synthesize Ag nanowires.^[108] After further complexation/photoreduction cycles, the metal clusters on the DNA templates became larger and showed increased polydispersity. In another study by Berti et al. for the photoreduction of silver ions on DNA templates, 254 nm ultraviolet light was used to irradiate the complexes of DNA-Ag⁺ followed by electroless deposition of nickel.^[109] Metal growth occurred mainly on DNA templates, with negligible background metal deposition. Several other metals, such as Au,^[110,111] Fe,^[112] Pd,^[113] Pt,^[76] and alloys,^[114] have been utilized to fabricate DNA-templated metal nanowires via photoreduction. Figure 7A shows TEM images of DNA-templated Au nanoclusters synthesized by photoreduction.^[111] In this work, the metallization of Au on DNA templates was limited to the discrete nanoclusters because of the limited Au available for each DNA chain. In Figure 7B, DNA-templated Au nanowires of different sizes were assembled by UV irradiation by varying DNA concentration with HAuCl₄ under the same conditions.^[115] Photoreduction using 260 nm UV light also allowed the synthesis of DNA-templated bimetallic nanowires by simultaneous reduction of both Ag and Au on DNA molecules as shown in Figure 7C.^[114] 260 nm UV light is also capable of releasing S²⁻ from thioacetamide; therefore, the S²⁻ can interact with Cd(ClO₄)₂ and DNA templates to form DNA-templated CdS nanowires.^[116]

The photoreduction mechanism remains unclear. A hypothesis is that strong UV absorption enabled DNA molecules to act as photosensitizers to accelerate the photoreduction of metal ions by facilitating electron transfer, thereby resulting in the photooxidation of DNA templates.^[76,110] Various organic agents, such as poly(vinyl) alcohol^[117] and ethylene glycol,^[118] can also accelerate the photoreduction of metal ions under UV light. Solvents and buffer salts play vital roles in electron transfer for photoreduction.^[119] However, further studies are necessary to elucidate the entire photoreduction mechanism of metal ions on DNA templates. The main advantage of the photoreduction approach is the low background nanomaterial generation that assists most metals in growing homogeneously on DNA templates. Another advantage is that it is a simple and rapid method that does not require the addition of reducing agents. UV irradiation facilitates the sugar moieties of the DNA to generate hydroxyl radicals which reduce metal ions on the DNA templates. On the other hand, UV irradiation may cause DNA damage in DNA-templated nanowire products.^[91,120]

3.1.4. Microwave Heating

In addition to traditional methods of inducing metal growth in DNA, such as UV irradiation, microwave heating has emerged as a powerful and efficient technique for metallizing DNA.^[59] Microwave heating is capable of inducing a rapid and localized increase in temperature, which can lead to the deposition of metal ions onto DNA molecules and subsequent growth of metallic structures. In this case, the DNA functions as a capping and reducing agent without requiring other additives. During

microwave heating, the heat energy of the microwave to the dielectrics leads to the immediate and fast deposition of metal NPs on DNA templates.

The important advantages of the microwave approach are uniform heating and fast formation of DNA-templated metal nanowires. Kundu et al. used a microwave heating approach to fabricate DNA-templated CdS nanowires.^[61] Most methods use micelles, surfactants, high molecular weight nitrogen-containing ligands, or phosphorus-containing ligands to stabilize the CdS NPs; however, these components can decrease the purity of DNA-templated CdS nanowires. Microwave heating has several advantages, such as enhanced reaction rates and the selective heating of dielectrics. Furthermore, microwave heating approaches offer flexibility, short reaction times, rapid nucleation of metal ions, and simplicity. In one study, only 60 s of microwave irradiation was required to synthesize conductive DNA-templated CdS nanowires.^[61] Kundu et al. also synthesized DNA-templated TiO₂ nanowires by microwave heating.^[72] Nithiyantham et al. used a microwave heating approach to synthesize DNA-templated Os nanowires by microwave irradiation on a mixture of DNA templates and Os ions in the presence of ethanol functioning as reducing agents as shown in Figure 8A.^[121] The metal growth of Au by microwave heating is fast and simple as shown in Figure 8B;^[59] however, it is important to maintain the stability of the DNA templates under microwave irradiation. The optimum microwave irradiation times and DNA concentrations affect the stabilities of product solutions. Compared with photoreduction, microwave heating is faster. In general, UV-photoreduction takes 4–6 h; on the other hand, microwave heating takes approximately 60 s.^[61,121]

3.2. DNA Metallization via Chemically Modified DNA

DNA nanowires formed by electrostatic interactions are randomly metalized and have irregular shapes and diameters. One solution to control the homogeneity and size-tunability of nanowires is to chemically modify DNA to include reducing groups that selectively react with the metal ions, forming consistent metal clusters for further controlled growth. The general principle behind obtaining DNA-templated nanowires using the DNA modification technique involves the introduction of reducing groups (azide/aldehyde) that can react with metal ions (Tollen's solution) via redox reactions to form metal clusters.

Keren et al. introduced an aldehyde group to adenine with glutaraldehyde, which acted as a reducing site for silver.^[79,122] Each aldehyde group reduced two silver ions. The size of these metal clusters was controlled by varying the number of reducing groups on the DNA strand based on redox reaction stoichiometry. In addition, Wirges et al. demonstrated that dialdehyde-modified DNA forms a larger number of chain-like silver clusters.^[123]

In addition to aldehydes, DNA modified with alkynes is another platform for nanowire synthesis. The alkyne groups on DNA were further derivatized via click chemistry, resulting in a metalized-sensitive functional group.^[88,124] After adding Tollens reagent as a reductant and a gold enhancement solution (HAuCl₄ and KSCN), bimetallic nanowires of Au–Ag formation were observed, as shown in Figure 9A.^[78] A major advantage of this approach was the control of the diameters and aspect ratios of the wires. Moreover, the nanowires obtained using this

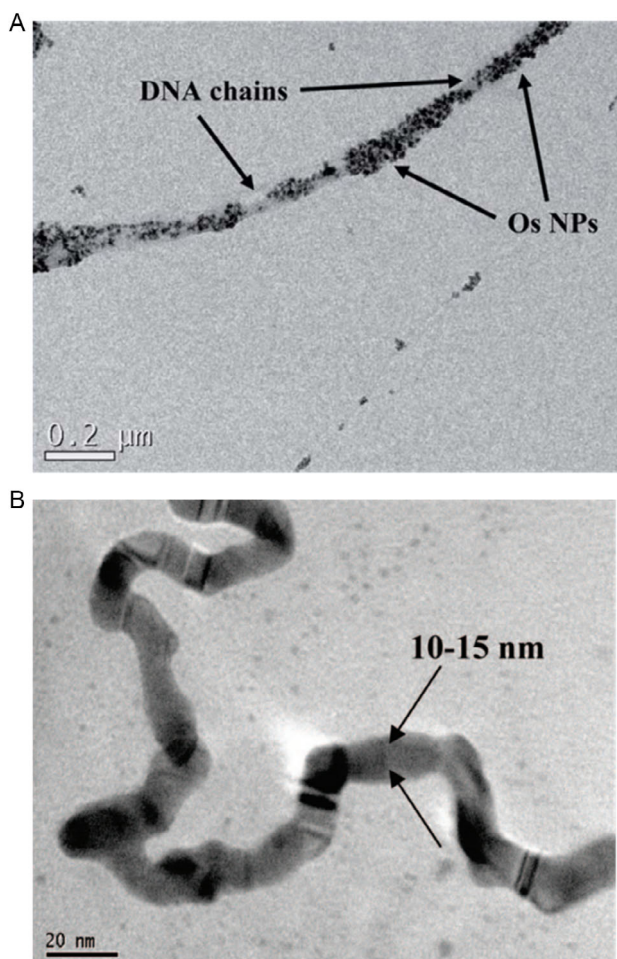


Figure 8. DNA-templated nanowires assembled by heating. A) Os nanowire assembly with microwave irradiation. 20 s of microwave heating formed DNA-templated Os nanowires. Reproduced with permission.^[121] Copyright 2014, RSC. B) DNA-templated Au nanowires. 180 s of microwave exposure generated a DNA-templated Au nanowires with diameters of approximately 10–15 nm. Reproduced with permission.^[59] Copyright 2008, ACS.

method were more homogeneous than those formed by electrostatic interactions.

Combining aldehyde and alkyne tag, a difunctional DNA template was also developed for the alkyne-dialdehyde DNA.^[125] The aldehyde group facilitated silver seed formation, and the alkyne groups were instrumental in attaching the DNA onto an azide-modified substrate via click chemistry. Upon further deposition of Au for 50 s, a 2.32 μm long DNA wire was obtained with a uniform 80 nm diameter and reasonable ohmic behavior.

Figure 9B illustrates the AuNP-bound DNA molecules.^[126] Colloidal AuNPs were stabilized with glutathione-bisazide via Au-thiol chemistry. Thus, upon adding the azide-modified AuNPs to the alkyne-modified DNA, 1D equidistantly arranged AuNPs were obtained via click chemistry in the presence of a Cu(I) catalyst. Unlike continuous nanowires, colloidal AuNPs were spaced at intervals, influenced by the design of the DNA template and the size of the ligand shell. Stearic hindrance

between the ligand shells of adjacent AuNPs produced a consistent interparticle distance of 2.8 ± 0.5 nm. In addition, the diameter of the nanowires can be modified by simply changing the size of the AuNPs.

The phosphate group in the DNA backbone can be modified using phosphorothioate (PS-DNA). Figure 9C illustrates an example of a bifunctional cross-linker with an alkanethiol (Au binding) and an iodoacetamide group (PS binding).^[127] DNA templates with PS modifications at defined locations assembled AuNPs at precisely defined positions. A biotin group can also be introduced on the bifunctional linker, which mediates the attachment of streptavidin-tagged AuNPs onto PS-DNA. While the thiol linker is restricted to AuNPs, a larger set of AuNPs can be easily modified with streptavidin, allowing the applicability of the biotin linker to a wider AuNP range.^[128]

In addition to phosphorothioate modification, the nonbridging oxygen of the phosphate backbone has been modified with a BH_3 group to obtain borane phosphate DNA (bp DNA). As the BH_3 group is a known reducing agent, it has been exploited for in situ metal reduction.^[129] While the applicability of bp DNA to obtain linear DNA nanowires has not been elucidated yet, silver nanoassemblies on 2D DNA origami crossover tiles^[130] and silver NP formation on carbon nanotube-wrapped bp DNA have been reported.^[131] Both PS-DNA and bp DNA provide higher stability to DNA, rendering it more reactive; however, the synthesis of long backbone-modified DNA remains challenging and therefore has limited applicability.

3.3. DNA Metallization Using DNA Intercalators

DNA-intercalating molecules are popular DNA-staining dyes, such as ethidium bromide, and TOTO-series including YOYO-1 and TOTO-1, SOTOX-R, and many others, which are widely used for fluorescence microscopy. They are a class of planar heterocyclic compounds resembling the ring structure of nucleic acid base pairs, allowing for their efficient insertion between stacked DNA bases. Similarly, Metallointercalators are widely used for DNA metallization applications and typically consist of a DNA-intercalating ligand that orients parallel to the base pairs via π -stacking. Thus, it acts as a stable anchor connected via a metal center to an ancillary ligand protruding from the DNA duplex.^[132]

Naphthalene diimide (NDI) is a threading intercalator that has been used for the formation of silver and gold nanowires. NDI is chemically modified to bear a galactose moiety at either end, which, upon the addition of Tollen's reagent, acts as the reducing group core to mediate the formation of silver ion precipitates on the DNA templates (silver mirror reaction) (Figure 10A). Further, gold nanowires are formed using silver nanowires as a template using λ DNA by the addition of a gold enhancement solution (HAuCl_4 and KSCN) with hydroquinone reduction.^[133] A particular advantage of using NDIs or intercalators is that they cannot bind to single-strand DNA (ssDNA) and thus can be used for the preferential metallization of dsDNA.^[134] The linker length between NDI and galactose plays a vital role in determining its binding affinity, and a longer linker was found to be more effective.^[133]

Figure 10B shows cisplatin (cis-Pt), a metal-containing small DNA-intercalating molecule that preferentially binds to poly G

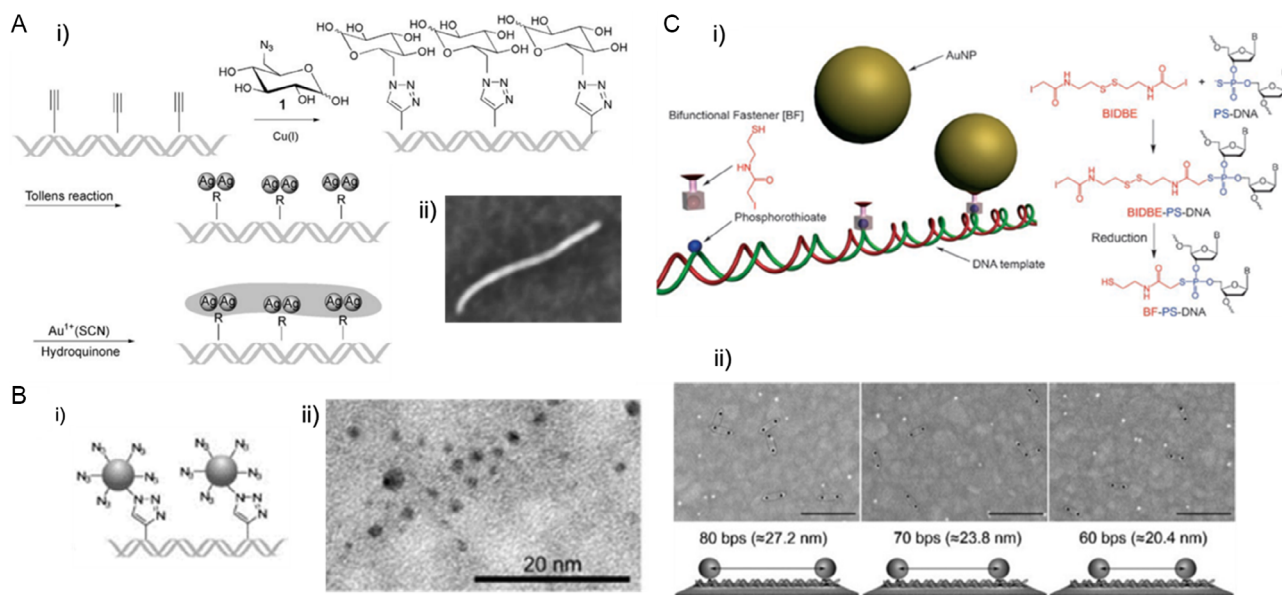


Figure 9. Metallization via DNA template modification. A) Click chemistry mediated by alkyne-modified DNA backbone. AFM image of Ag–Au bimetallic DNA nanowire. Reproduced with permission.^[78] Copyright 2007, Wiley-VCH. B) AuNPs on alkyne-modified DNA templates (TEM image). Reproduced with permissions.^[126] Copyright 2008, RSC. C) Bifunctional cross-linker mediated attachment of AuNPs onto phosphorothioate-modified DNA backbone. SEM images of AuNP assembled on DNA at defined inter-NP distances. Reproduced with permission.^[127] Copyright 2007, Wiley-VCH.

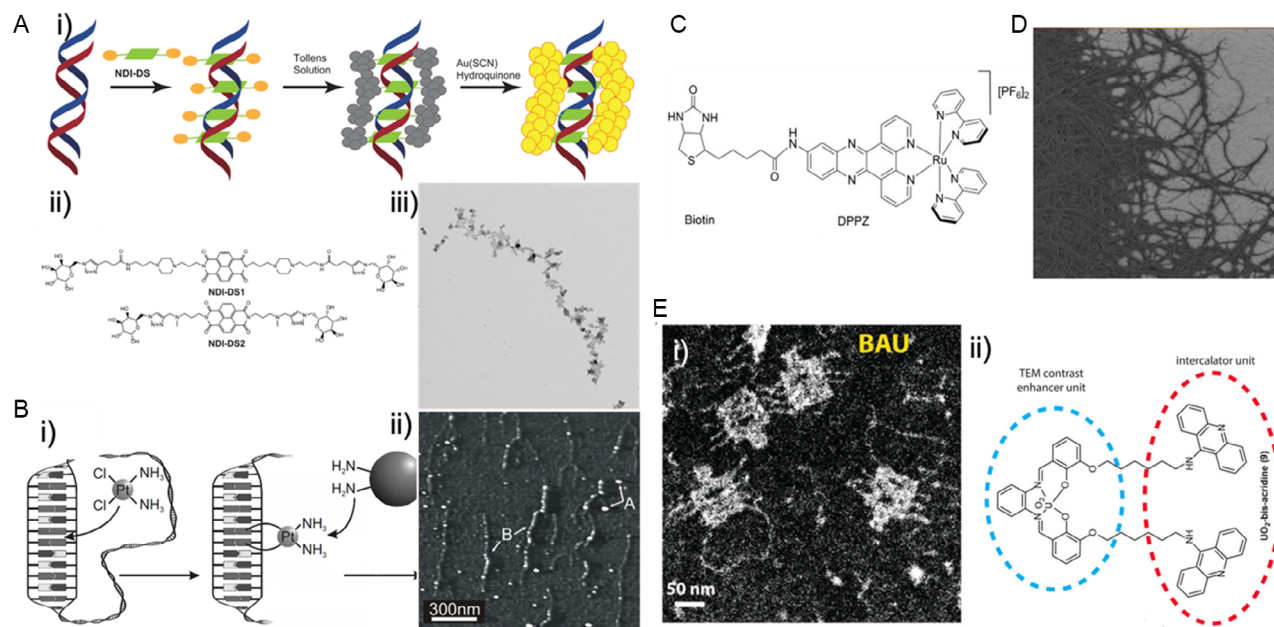


Figure 10. Metallization using reducing group modified DNA intercalators. A) Interactions of naphthalene diimide and DNA molecules. i) General scheme for the formation of metallic nanowires onto DNA complexed with naphthalene diimide followed by reduction with Tollens' reagent. ii) Chemical structure of naphthalene diimide. iii) TEM image of a DNA nanowire. Reproduced with permission.^[133] Copyright 2014, ACS. B) Interactions of cis-platin and DNA molecules. i) Scheme of interactions between cis-platin and DNA templates. ii) Image of Au nanoparticle-bound DNA molecules. Reproduced with permission.^[135] Copyright 2006, Springer. C) Structure of the intercalating agent ruthenium–DPPZ–biotin used to bind streptavidin-tagged AuNPs. Reproduced with permission.^[139] Copyright 2007, Wiley-VCH. D) SEM image of silver nanofibrils formed upon treatment of Ag–phen to DNA. Reproduced with permission.^[140] Copyright 2017, MDPI. E) i) Representative TEM image of DNA origami stained via bis-acridine uranyl ii) Reproduced with permission.^[142] Copyright 2019, Wiley-VCH.

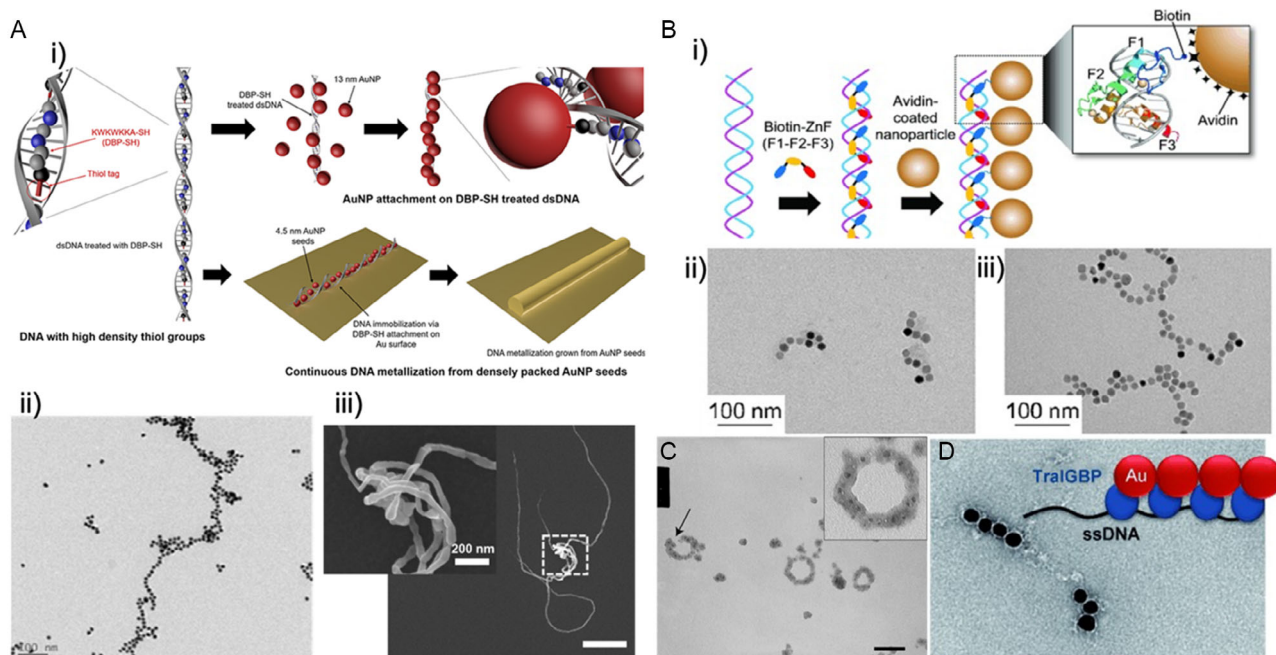


Figure 11. Metallization through DNA–peptide/protein interactions. A) The synthesis of gold nanowires using DNA-binding peptides: i) DBP-thiol (KWKWKKA) for the formation of DNA-templated Au nanowires; ii) SEM image of DNA nanowires formed by assembly of 13 nm AuNPs using DBPs; iii) TEM image of metallized Au nanowires on a stretched DNA template (inset—visualization of DNA in its 3D conformation). Reproduced with permission.^[90] Copyright 2016, Wiley-VCH. B) The assembly of gold nanoparticles into necklace-like structures using zinc finger proteins (ZnF) on DNA: i) schematic on utilizing ZnF–biotin for the assembly of avidin-coated AuNPs onto DNA; ii,iii) representative TEM images of AuNP assembly on DNA templates of different lengths, 437 bp (ii) and 809 bps (iii). Reproduced with permission.^[150] Copyright 2015, Wiley-VCH. C) TEM images of Cu₂O NPs self-organized on a circular DNA template using Tral with a Cu₂O-binding motif. Reproduced with permission.^[151] Copyright 2005, ACS. D) TEM image of AuNP assembly on Tral-GBP1-modified ssDNA template. Reproduced with permission.^[152] Copyright 2010, Wiley-VCH.

sequences. Thus, the addition of cis-Pt to DNA introduced amine groups into the guanine bases of DNA (Figure 11B-(i)). This has been exploited for the attachment of cysteamine-modified AuNPs to DNA via ligand exchange between the amine groups of AuNPs and the amine ligands of cis-Pt.^[135] Figure 11B-(ii) illustrates linearized DNA templates that bind to multiple AuNPs.^[136] In addition to the use of the cis-Pt amine groups, Pt is a good catalyst used to mediate the electrodeless deposition of silver on cis-Pt-treated DNA templates, forming long silver nanowires.^[137] The same group used block co-polymers of DNA to demonstrate that Pt metal was only detected in guanine-rich regions but was absent in other regions when analyzed via AFM, further validating the very high sequence specificity for binding of cis-Pt.^[68,138]

Figure 1C shows an intercalating agent (DPPZ) combined with a biotin moiety.^[139] Ruthenium-bound DPPZ luminesces upon DNA binding ($[\text{Ru}(\text{dppz})_2(\text{phen-biotin})_2][\text{PF}_6]_2$). This complex could bind to streptavidin-tagged AuNPs. Figure 10D shows long silver nanofibrils based on an intercalating agent of 1,10-phenanthroline, which formed coordination complexes with silver and DNA.^[140] 1,10-phenanthroline stabilized the complexes of silver-Phen-DNA.

Figure 10E shows the DNA-intercalating electron dye-containing uranyl acetate. Uranyl acetate is a dye commonly used to stain DNA by binding to the DNA backbone, with uranium acting as an

efficient electron scatterer.^[141] By combining the electron scattering property of uranyl acetate with that of a DNA intercalating group, Kabiri et al. developed a novel DNA staining agent, bis-acridine uranyl (BAU) (Figure 11E).^[142] BAU contains two acridine heterocycles covalently linked to uranium via salophen-type coordination chemistry, allowing for tweezer-like binding to DNA. This reagent is useful for visualizing DNA under EM because it improves the contrast of the stained DNA from the background, which is comparable to that of uranyl acetate.

3.4. DNA Metallization Using DNA-Binding Peptide/Protein

Various peptides and proteins can bind to DNA with natural affinity, termed DNA-binding peptides/proteins (DBPs).^[143,144] In biological systems, these fall under a broad family of chromosomal proteins and transcription factors, which bind to DNA and regulate gene expression. Given their natural affinity for DNA, DBPs are promising anchors for DNA nanowire generation via noncovalent biological interactions. Unlike chemical intercalators with limited tailoring ability, DBPs can be precisely designed to have the desired physicochemical properties by simply tweaking their amino acid constituents because the peptide sequence defines its function. These DBPs can also be engineered to contain metal-binding motifs. A review summarized many kinds of NP-binding peptides.^[145] In addition, with the

advances in genetic engineering, these peptides can be easily cloned, synthesized, and purified at a laboratory scale within a few days.

In the context of DNA visualization, DBPs have been designed to bind DNA either sequence-specifically or independently. Sequence-independent binding DBPs are synthetic polycationic peptides that interact electrostatically with the polyanionic phosphate backbone of DNA. One such example is the (KW)_n subunit, where the electrostatic binding of lysine (K) is complemented by the intercalation of the aromatic ring in the tryptophan (W) residue rendering binding affinities comparable with those of organic DNA-intercalating dyes.^[143] On the other hand, sequence-dependent binding DBPs are generated using natural DNA-binding motifs such as tailorable zinc finger (ZnF), transcription-activator-like effectors (TALE), and HMG (high mobility group)/H-NS (histone-like nucleoid structural protein) which have inherent preferential binding to A/T-rich regions.^[146,147] These have thus far been coupled to fluorophores for A/T-specific DNA visualization via fluorescence microscopy.^[148]

Figure 11A shows DNA-bound peptide-linked AuNPs.^[90] Given that this peptide had DNA-binding affinity, the assembly of 13 nm colloidal AuNPs onto a λ DNA template was shown in Figure 11A-(ii). As DBP-SH was found to bind through the entire length of the DNA homogeneously, they exploited this to visualize the DNA backbone in its native form using seed-mediated growth of AuNPs to obtain uniform metallic nanowires. The DBP-SH-coated DNA was treated with a 4.5 nm AuNP seed solution followed by a growth solution consisting of ascorbic acid. The seed-mediated growth produced smooth and continuous DNA nanowires with a constant diameter for direct visualization of DNA in its native 3D conformation, as evidenced by SEM (Figure 11A-(iii)). This concept has been extended to obtain multifunctional nanoassemblies of AuNPs, quantum dots, and magnetic NPs (Fe₃O₄) on CNT-wrapped DNA templates.^[149]

Figure 11B demonstrates a biotin-conjugated zinc finger that binds DNA sequence specifically.^[150] Notably, by varying the number of fingers and the linkers between the fingers, the zinc fingers were tailored to have variable sequence specificity and affinity to DNA.^[147] As a proof-of-concept, Ryu et al. modified Cys₂-His₂ zinc-finger QNKQKRHR (which shows sequence-specific binding to the nucleic acid sequence GAGGCAGAA) with biotin for the binding of avidin-coated magnetic particles onto pre-designed dsDNA templates.

Proteins can also be designed to contain NP-binding motifs. One such example was the DNA-binding protein TraI (Figure 11C). It consists of relaxase and helicase domains. The relaxase domain has a sequence-specific ssDNA-binding affinity, and the helicase domain has a nonspecific dsDNA-binding affinity. Dai et al. engineered it with a Cu₂O-binding motif CN225 (RHTDGLRRIAAR) at the N-terminus of the protein.^[151] They visualized circular bacteriophage dsDNA, where NP-decorated loops could be observed via TEM, as shown in Figure 11C. As an extension to this study, they also modified TraI with a 7X-tandem repeat of a gold-binding peptide motif (MHGKTQATSGT IQS) at an internal site of the protein to avoid loss of the NP-binding domain via degradation if present in the terminal.^[152] Figure 11D shows the binding of AuNPs onto both ssDNA and dsDNA templates.

3.5. Metal Labeling toward Sequence-Specific EM Images

Conjugation of proteins such as antibodies (immunoelectron microscopy) and enzymes with gold is a popular technique used for studying nucleic acid localization in cells. In the antibody-based labeling method (immunogold), the anti-DNA primary antibody is treated with a gold-conjugated secondary antibody, facilitating the study of ultrastructural DNA localization in cells via visualization of Au clusters.^[153] To specifically identify the localization of replicated DNA, Thiry et al. developed the nucleobase BUdR (5-bromodeoxyuridine) for immunogold-based staining. In this method, BUdR is incorporated particularly in the replicating DNA either within the nucleolus of tumor cells or the different cellular organelles, which is identified using an anti-BUdR primary antibody followed by gold-conjugated secondary antibody.^[154] However, this method requires a specialized embedding and fixation of the biological sample, which can destruct its ultrastructural properties, resulting in poor distinction of the nucleolar compartments.^[155] Hence, TdT was combined with the BUdR-based immunogold staining to develop a powerful method that can be used to identify DNA in the various fibrillary components in the nucleolus of cells via EM.^[155,156]

By conjugation of enzymes such as DNase I or RNase A with colloidal AuNPs, localization of DNA and RNA, respectively, in tissue sections can be accurately determined at an EM level resolution.^[157] The *in situ* DNA hybridization has been expanded to EM-based detection (EM-ISH) where biotin-labeled short probe DNA hybridizes with the biological specimen, and streptavidin conjugated with gold is added for labeling the regions of hybridization. Upon silver staining, EM is used to identify the location of DNA with a specific sequence in the sample, as illustrated in Figure 12A.^[158]

Expanding on the BUdR strategy for labeling replicating DNA, direct nucleic acid modification with heavy metals is a more powerful method that has recently been applied for EM-based DNA sequencing. In one such attempt, dUTP was modified to contain mercury in the nitrogenous base, which, as shown in Figure 12B, allowed it to undergo template-dependent DNA polymerization to produce a Hg-decorated dsDNA strand in the location of adenine, which can be visualized by EM.^[159] Along similar lines, dGTP was modified to include platinum, facilitating the identification of cytosine in the template DNA (Figure 12D).^[160] While individual bases have been modified in the above studies as a proof-of-concept, multiplexing with different contrast-agent labels in combination with a high-resolution automated imager allows for direct DNA sequencing from EM-based images, as demonstrated by Own et al., shown in Figure 12C.^[161]

4. Conclusion

This review summarizes various DNA staining methods for EM and highlights their advantages and limitations for visualizing genomic DNA. The first method for DNA imaging using EM was shadow casting of heavy metals in 1948. Since 1961, the use of uranyl acetate staining combined with platinum shadowing has been widespread in the field of DNA visualization and has been used in a wide range of studies to reveal the structure and organization of DNA molecules under EM.

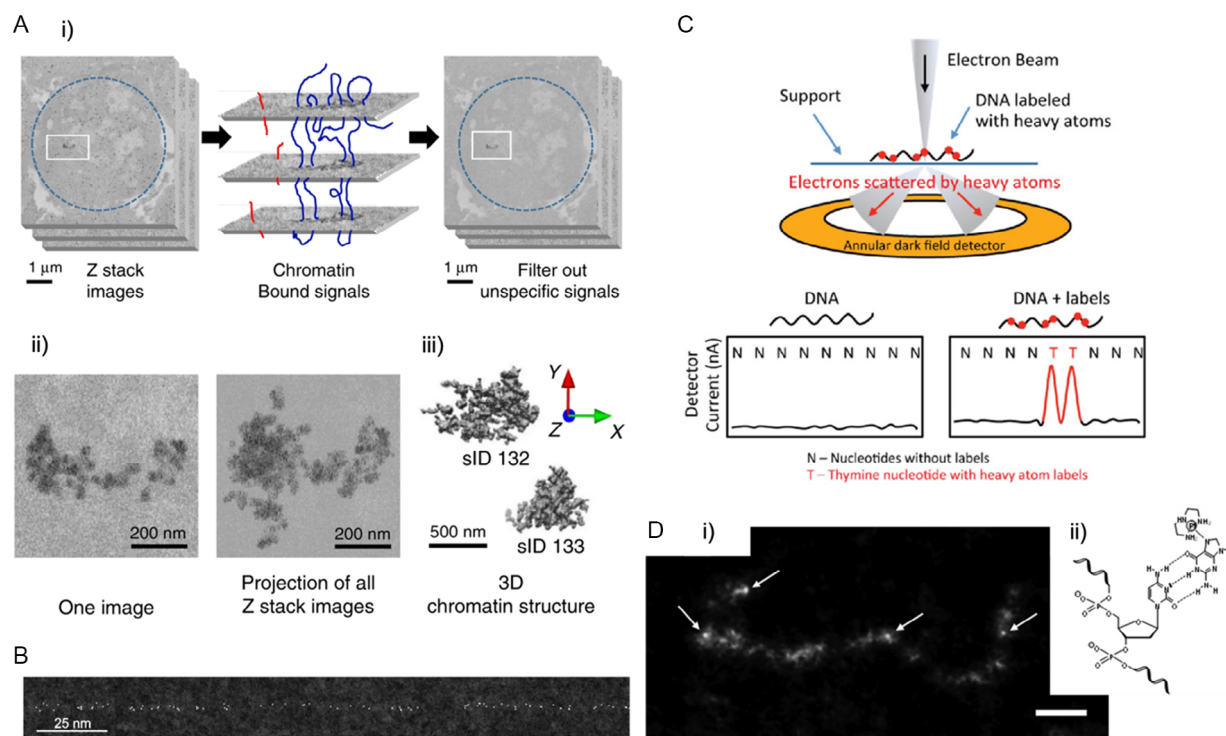


Figure 12. Sequence-specific labels under EM. A) Schematic of the 3D reconstruction of chromatin architecture using EM-ISH. Reproduced with permission.^[158] Copyright 2020, Springer Nature. B) EM image of osmium-labeled ssDNA. Reproduced with permission.^[161] Copyright 2013, Oxford University Press. C) The principle behind heavy atom-based labeling of DNA and read-out thereof. Reproduced with permission.^[159] Copyright 2012, Oxford University Press. D) EM image of Pt-modified adenine-labeled DNA. Reproduced with permission.^[160] Copyright 2016, Wiley-VCH.

In addition to uranium, other heavy metals have also been used to stain DNA molecules for EM, including lanthanum, osmium, hafnium, tungsten, and platinum. These heavy metals have different properties and can offer unique advantages for DNA staining and imaging, including high contrast, specificity, and resolution. However, each metal has its own drawbacks, including toxicity, radioactivity, and limited availability for imaging. Uranium is generally recognized as providing the highest image quality, due to its high electron density and low background noise. However, due to its radioactivity and toxicity, it requires strict government regulations for its use. Furthermore, uranyl acetate-stained DNA is only suitable for TEM, and not SEM.

To address these limitations, researchers have developed nanomaterial-based DNA staining methods using nanoparticles and nanowires. These materials are safe and easily visible under both TEM and SEM. In general, positively charged nanoparticles or metal ions electrostatically interact with negatively charged DNA molecules. These nanoparticles can then be grown into nanowires via chemical reduction, electrochemical reduction, photoreduction, or heating, allowing for the visualization of DNA at the nanoscale. Alternatively, nanoparticle-bound DNA-binding peptide motifs or DNA intercalators can be used as seeds for nanowire growth, providing a powerful tool for the visualization and analysis of DNA–protein interactions. In addition, BUdR (5-bromouridine) nanoparticle labeling and EM-optimized fluorescence in situ hybridization (EM-ISH) were developed as

promising approaches for achieving sequence-specific DNA visualization.

In conclusion, the use of heavy metals and nanoparticles for DNA staining and imaging under EM represents an important platform for the development of advanced nanotechnology and has the potential to transform our understanding of the structure, organization, and function of DNA molecules, and its interaction with proteins. These tools have potential applications in a wide range of fields, including nanoelectronics, biosensing, and biomedicine.

Acknowledgements

X.J. and S.K. contributed equally to this work. All authors contributed to the manuscript writing and figures. All authors have approved the final version of the manuscript. This study was supported by the Samsung Research Funding Center (SRFC-MA2101-07).

Conflict of Interest

The authors declare no conflict of interest.

Keywords

DNA–peptide/protein interactions, electron microscope, genomic DNA visualizations, heavy metal staining, nanoparticle staining, nanowire metallization

Received: November 23, 2022

Revised: February 20, 2023

Published online:

- [1] a) F. Sanger, S. Nicklen, A. R. Coulson, *Proc. Natl. Acad. Sci. U.S.A.* **1977**, *74*, 5463; b) A. M. Maxam, W. Gilbert, *Proc. Natl. Acad. Sci. U.S.A.* **1977**, *74*, 560.
- [2] a) M. Margulies, M. Egholm, W. E. Altman, S. Attiya, J. S. Bader, L. A. Bemben, J. Berka, M. S. Braverman, Y. J. Chen, Z. T. Chen, S. B. Dewell, L. Du, J. M. Fierro, X. V. Gomes, B. C. Godwin, W. He, S. Helgesen, C. H. Ho, G. P. Irzyk, S. C. Jando, M. L. I. Alenquer, T. P. Jarvie, K. B. Jirage, J. B. Kim, J. R. Knight, J. R. Lanza, J. H. Leamon, S. M. Lefkowitz, M. Lei, J. Li, K. L. Lohman, et al., *Nature* **2005**, *437*, 376; b) D. R. Bentley, S. Balasubramanian, H. P. Swerdlow, G. P. Smith, J. Milton, C. G. Brown, K. P. Hall, D. J. Evers, C. L. Barnes, H. R. Bignell, J. M. Boutell, J. Bryant, R. J. Carter, R. K. Cheetham, A. J. Cox, D. J. Ellis, M. R. Flatbush, N. A. Gormley, S. J. Humphray, L. J. Irving, M. S. Karbelashvili, S. M. Kirk, H. Li, X. H. Liu, K. S. Masinger, L. J. Murray, B. Obradovic, T. Ost, M. L. Parkinson, M. R. Pratt, et al., *Nature* **2008**, *456*, 53.
- [3] a) M. Jain, S. Koren, K. H. Miga, J. Quick, A. C. Rand, T. A. Sasani, J. R. Tyson, A. D. Beggs, A. T. Dilthey, I. T. Fiddes, S. Malla, H. Marriott, T. Nieto, J. O'Grady, H. E. Olsen, B. S. Pedersen, A. Rhie, H. Richardson, A. R. Quinlan, T. P. Snutch, L. Tee, B. Paten, A. M. Phillippy, J. T. Simpson, N. J. Loman, M. Loose, *Nat. Biotechnol.* **2018**, *36*, 338; b) A. M. Wenger, P. Peluso, W. J. Rowell, P. C. Chang, R. J. Hall, G. T. Concepcion, J. Ebler, A. Functammasan, A. Kolesnikov, N. D. Olson, A. Topfer, M. Alonge, M. Mahmoud, Y. Qian, C. S. Chin, A. M. Phillippy, M. C. Schatz, G. Myers, M. A. DePristo, J. Ruan, T. Marschall, F. J. Sedlazeck, J. M. Zook, H. Li, S. Koren, A. Carroll, D. R. Rank, M. W. Hunkapiller, *Nat. Biotechnol.* **2019**, *37*, 1155.
- [4] S. Nurk, S. Koren, A. Rhie, M. Rautiainen, A. V. Bzikadze, A. Mikheenko, M. R. Vollger, N. Altemose, L. Uralsky, A. Gershman, S. Aganezov, S. J. Hoyt, M. Diekhans, G. A. Logsdon, M. Alonge, S. E. Antonarakis, M. Borchers, G. G. Bouffard, S. Y. Brooks, G. V. Caldas, N. C. Chen, H. Cheng, C. S. Chin, W. Chow, L. G. de Lima, P. C. Dishuck, R. Durbin, T. Dvorkina, I. T. Fiddes, G. Formenti, et al., *Science* **2022**, *376*, 44.
- [5] V. Marx, *Nat. Methods* **2023**, *20*, 6.
- [6] a) S. Goodwin, J. D. McPherson, W. R. McCombie, *Nat. Rev. Genet.* **2016**, *17*, 333; b) C. Alkan, S. Sajjadian, E. E. Eichler, *Nat. Methods* **2011**, *8*, 61.
- [7] G. Huszka, M. A. M. Gijs, *Micro Nano Eng.* **2019**, *2*, 7.
- [8] J. F. Scott, *Biochim. Biophys. Acta* **1948**, *2*, 1.
- [9] a) C. E. Hall, *Proc. Natl. Acad. Sci. U.S.A.* **1956**, *42*, 801; b) Y. Fujiyoshi, N. Uyeda, *Ultramicroscopy* **1981**, *7*, 189.
- [10] J. D. Griffith, *Science* **1975**, *187*, 1202.
- [11] R. C. Williams, *Proc. Natl. Acad. Sci. U.S.A.* **1977**, *74*, 2311.
- [12] C. R. Zobel, M. Beer, *J. Biophys. Biochem. Cytol.* **1961**, *10*, 335.
- [13] C. Brack, *CRC Crit. Rev. Biochem.* **1981**, *10*, 113.
- [14] R. C. Williams, R. W. G. Wyckoff, *J. Appl. Phys.* **1944**, *15*, 712.
- [15] G. M. Hendricks, *Methods Mol. Biol.* **2014**, *1117*, 73.
- [16] A. K. Kleinschmidt, D. Lang, D. Jacherts, R. K. Zahn, *Biochim. Biophys. Acta* **1962**, *61*, 857.
- [17] R. W. Davis, N. Davidson, *Proc. Natl. Acad. Sci. U.S.A.* **1968**, *60*, 243.
- [18] J. Dubochet, M. Ducommun, M. Zollinger, E. Kellenberger, *J. Ultrastruct. Res.* **1971**, *35*, 147.
- [19] A. G. Harford, M. Beer, *J. Mol. Biol.* **1972**, *69*, 179.
- [20] C. Brack, V. Pirrotta, *J. Mol. Biol.* **1975**, *96*, 139.
- [21] a) A. K. Kleinschmidt, *Philos. Trans. R. Soc. London, B* **1971**, *261*, 143; b) C. Brack, H. Eberle, T. A. Bickle, R. Yuan, *J. Mol. Biol.* **1976**, *104*, 305.
- [22] a) R. B. Inman, *Methods in Enzymology*, Vol. 29, Academic Press, Waltham, MA **1974**, p. 451; b) R. B. Inman, M. Schnos, *J. Mol. Biol.* **1970**, *49*, 93.
- [23] C. T. Beck, S. Schwinn, H. Zentgraf, *Chromosoma* **1995**, *103*, 653.
- [24] S. Fakan, S. P. Modak, *Exp. Cell. Res.* **1973**, *77*, 95.
- [25] S. M. Berget, C. Moore, P. A. Sharp, *Proc. Natl. Acad. Sci. U.S.A.* **1977**, *74*, 3171.
- [26] M. R. Inciarte, M. Salas, J. M. Sogo, *J. Virol.* **1980**, *34*, 187.
- [27] a) P. Oudet, M. Gross-Bellard, P. Chambon, *Cell* **1975**, *4*, 281; b) J. Bednar, R. A. Horowitz, S. A. Grigoryev, L. M. Carruthers, J. C. Hansen, A. J. Koster, C. L. Woodcock, *Proc. Natl. Acad. Sci. U.S.A.* **1998**, *95*, 14173.
- [28] a) G. Christiansen, J. Griffith, *Proc. Natl. Acad. Sci. U.S.A.* **1986**, *83*, 2066; b) J. Flory, S. S. Tsang, K. Muniyappa, *Proc. Natl. Acad. Sci. U.S.A.* **1984**, *81*, 7026.
- [29] a) A. K. Kleinschmidt, D. Lang, D. Jacherts, R. K. Zahn, *Biochim. Biophys. Acta, Spec. Sect. Nucleic Acids Relat. Subj.* **1962**, *61*, 857; b) L. A. Machattie, C. A. Thomas Jr., *Science* **1964**, *144*, 1142; c) D. Stuber, H. Bujard, *Mol. Gen. Genet.* **1977**, *154*, 299.
- [30] S. Mijic, R. Zellweger, N. Chappidi, M. Berti, K. Jacobs, K. Mutreja, S. Ursich, A. Ray Chaudhuri, A. Nussenzweig, P. Janscak, M. Lopes, *Nat. Commun.* **2017**, *8*, 859.
- [31] L. Olavarrieta, M. L. Martinez-Robles, J. M. Sogo, A. Stasiak, P. Hernandez, D. B. Krimer, J. B. Schwartzman, *Nucleic Acids Res.* **2002**, *30*, 656.
- [32] K. Koberna, A. Ligasova, J. Malinsky, A. Pliss, A. J. Siegel, Z. Cvackova, H. Fidlerova, M. Masata, M. Fialova, I. Raska, R. Berezney, *J. Cell. Biochem.* **2005**, *94*, 126.
- [33] Y. Benureau, E. Moreira Tavares, A. A. Muhammad, S. Baconnais, E. Le Cam, P. Dupaigne, *Biol. Methods Protoc.* **2020**, *5*, bpaa012.
- [34] R. Zellweger, D. Dalcher, K. Mutreja, M. Berti, J. A. Schmid, R. Herrador, A. Vindigni, M. Lopes, *J. Cell Biol.* **2015**, *208*, 563.
- [35] Y. Benureau, C. Pouvelle, P. Dupaigne, S. Baconnais, E. Moreira Tavares, G. Mazon, E. Despras, E. Le Cam, P. L. Kannouche, *Nucleic Acids Res.* **2022**, *50*, 9909.
- [36] M. Fumasoni, K. Zwicky, F. Vanoli, M. Lopes, D. Branzei, *Mol. Cell.* **2015**, *57*, 812.
- [37] Z. Zhou, R. Yan, W. Jiang, J. M. K. Irudayaraj, *Nanoscale Adv.* **2021**, *3*, 1019.
- [38] T. Nikitina, D. Norouzi, S. A. Grigoryev, V. B. Zhurkin, *Sci. Adv.* **2017**, *3*, e1700957.
- [39] J. Jackson, A. Vindigni, *Methods Mol. Biol.* **2022**, *2444*, 81.
- [40] a) R. Zellweger, M. Lopes, *Methods Mol. Biol.* **2018**, *1672*, 261; b) M. Lopes, *Methods Mol. Biol.* **2009**, *521*, 605.
- [41] M. Kosar, D. Piccini, M. Foiani, M. Giannattasio, *Nucleic Acids Res.* **2021**, *49*, e121.
- [42] a) O. A. Kladova, M. Bazlekowa-Karaban, S. Baconnais, O. Pietrement, A. A. Ishchenko, B. T. Matkarimov, D. A. Iakovlev, A. Vasenko, O. S. Fedorova, E. Le Cam, B. Tudek, N. A. Kuznetsov, M. Saparbaev, *DNA Repair* **2018**, *64*, 10; b) V. M. Kissling, G. Reginato, E. Bianco, K. Kasaciunaite, J. Tilma, G. Cereghetti, N. Schindler, S. S. Lee, R. Guerois, B. Luke, R. Seidel, P. Cejka, M. Peter, *Nat. Commun.* **2022**, *13*, 2374.
- [43] S. Manger, U. H. Ermel, A. S. Frangakis, *Commun. Biol.* **2021**, *4*, 234.
- [44] M. Nakakoshi, H. Nishioka, E. Katayama, *J. Electron Microsc.* **2011**, *60*, 401.
- [45] M. D. Cole, J. W. Wiggins, M. Beer, *J. Mol. Biol.* **1977**, *117*, 387.
- [46] K. Ikeda, K. Inoue, S. Kanematsu, Y. Horiuchi, P. Park, *Microsc. Res. Tech.* **2011**, *74*, 825.
- [47] M. Egel-Mitani, R. Egel, Z. Naturforsch., B: Anorg. Chem., Org. Chem., Biochem., Biophys., Biol. **1972**, *27*, 480.

- [48] S. Inaga, T. Katsumoto, K. Tanaka, T. Kameie, H. Nakane, T. Naguro, *Arch. Histol. Cytol.* **2007**, *70*, 43.
- [49] S. Sato, A. Adachi, Y. Sasaki, M. Ghazizadeh, *J. Microsc.* **2008**, *229*, 17.
- [50] O. L. Miller Jr., B. R. Beatty, *Science* **1969**, *164*, 955.
- [51] a) L. Xie, Z. Liu, *Mol. Syst. Biol.* **2021**, *17*, e9653; b) D. P. Hoffman, G. Shtengel, C. S. Xu, K. R. Campbell, M. Freeman, L. Wang, D. E. Milkie, H. A. Pasolli, N. Iyer, J. A. Bogovic, D. R. Stablesy, A. Shirinifard, S. Pang, D. Peale, K. Schaefer, W. Pomp, C. L. Chang, J. Lippincott-Schwartz, T. Kirchhausen, D. J. Solecki, E. Betzig, H. F. Hess, *Science* **2020**, *367*, eaaz5357.
- [52] H. D. Ou, S. Phan, T. J. Deerinck, A. Thor, M. H. Ellisman, C. C. O'Shea, *Science* **2017**, *357*, eaag0025.
- [53] Y. Li, A. Eshein, R. K. A. Virk, A. Eid, W. Wu, J. Frederick, D. VanDerway, S. Gladstein, K. Huang, A. R. Shim, N. M. Anthony, G. M. Bauer, X. Zhou, V. Agrawal, E. M. Pujadas, S. Jain, G. Esteve, J. E. Chandler, T. Q. Nguyen, R. Bleher, J. J. de Pablo, I. Szleifer, V. P. Dravid, L. M. Almossalha, V. Backman, *Sci. Adv.* **2021**, *7*, eabe4310.
- [54] B. Hubner, E. von Otter, B. Ahsan, M. L. Wee, S. Henriksson, A. Ludwig, S. Sandin, *Nucleic Acids Res.* **2022**, *50*, 5047.
- [55] E. Braun, Y. Eichen, U. Sivan, G. Ben-Yoseph, *Nature* **1998**, *391*, 775.
- [56] J. Kondo, Y. Tada, T. Dairaku, Y. Hattori, H. Saneyoshi, A. Ono, Y. Tanaka, *Nat. Chem.* **2017**, *9*, 956.
- [57] S. Cui, Y. Liu, Z. Yang, X. Wei, *Mater. Des.* **2007**, *28*, 722.
- [58] T. Bayrak, S. Helmi, J. Ye, D. Kauert, J. Kelling, T. Schonherr, R. Weichelt, A. Erbe, R. Seidel, *Nano Lett.* **2018**, *18*, 2116.
- [59] S. Kundu, H. Liang, *Langmuir* **2008**, *24*, 9668.
- [60] S. N. Sarangi, B. C. Behera, N. K. Sahoo, S. K. Tripathy, *Biosens. Bioelectron.* **2021**, *190*, 113402.
- [61] S. Kundu, H. Lee, H. Liang, *Inorg. Chem.* **2009**, *48*, 121.
- [62] Q. Gu, D. T. Haynie, *Mater. Lett.* **2008**, *62*, 3047.
- [63] B. Uprety, E. P. Gates, Y. Geng, A. T. Woolley, J. N. Harb, *Langmuir* **2014**, *30*, 1134.
- [64] S. M. Watson, H. D. Mohamed, B. R. Horrocks, A. Houlton, *Nanoscale* **2013**, *5*, 5349.
- [65] Q. Gu, H. Jin, K. Dai, *J. Phys. D: Appl. Phys.* **2009**, *42*, 015303.
- [66] a) J. Richter, M. Mertig, W. Pompe, H. Vinzelberg, *Appl. Phys. A: Mater. Sci. Process.* **2002**, *74*, 725; b) J. Richter, M. Mertig, W. Pompe, I. Monch, H. K. Schackert, *Appl. Phys. Lett.* **2001**, *78*, 536.
- [67] J. Richter, R. Seidel, R. Kirsch, M. Mertig, W. Pompe, J. Plaschke, H. K. Schackert, *Adv. Mater.* **2000**, *12*, 507.
- [68] A. Tanaka, Y. Matsuo, Y. Hashimoto, K. Ijio, *Chem. Commun.* **2008**, *36*, 4270.
- [69] W. E. Ford, O. Harnack, A. Yasuda, J. M. Wessels, *Adv. Mater.* **2001**, *13*, 1793.
- [70] H. D. A. Mohamed, S. M. D. Watson, B. R. Horrocks, A. Houlton, *J. Mater. Chem. C* **2014**, *3*, 438.
- [71] J. Liu, B. Uprety, S. Gyawali, A. T. Woolley, N. V. Myung, J. N. Harb, *Langmuir* **2013**, *29*, 11176.
- [72] U. Nithyanantham, A. Ramadoss, S. R. Ede, S. Kundu, *Nanoscale* **2014**, *6*, 8010.
- [73] A. Bezryadin, P. M. Goldbart, *Adv. Mater.* **2010**, *22*, 1111.
- [74] a) N. C. Seeman, *J. Theor. Biol.* **1982**, *99*, 237; b) N. C. Seeman, *Angew. Chem. Int. Ed.* **1998**, *37*, 3220; c) N. C. Seeman, *Chem. Biol.* **2003**, *10*, 1151; d) F. Zhang, J. Nangreave, Y. Liu, H. Yan, *J. Am. Chem. Soc.* **2014**, *136*, 11198; e) J. Chao, Y. Zhang, D. Zhu, B. Liu, C. Cui, S. Su, C. Fan, L. Wang, *Sci. China Chem.* **2016**, *59*, 730; f) M. Xie, Y. Hu, J. Yin, Z. Zhao, J. Chen, J. Chao, *Research* **2022**, *2022*, 9840131; g) C. Pang, B. R. Aryal, D. R. Ranasinghe, T. R. Westover, A. E. F. Ehlert, J. N. Harb, R. C. Davis, A. T. Woolley, *Nanomaterials* **2021**, *11*, 1655; h) N. Li, Y. Shang, Z. Han, T. Wang, Z. G. Wang, B. Ding, *ACS Appl. Mater. Interfaces* **2019**, *11*, 13835; i) K. Ijio, H. Mitomo, *Polym. J.* **2017**, *49*, 815.
- [75] a) C. M. Niemeyer, *Angew. Chem. Int. Ed.* **2001**, *40*, 4128; b) J. Huang, L. Lin, D. Sun, H. Chen, D. Yang, Q. Li, *Chem. Soc. Rev.* **2015**, *44*, 6330.
- [76] B. Sun, L. Yang, M. Zhang, F. Meng, X. Chen, M. Li, J. Liu, *Mater. Res. Bull.* **2009**, *44*, 1270.
- [77] a) J. Richter, *Phys. E* **2003**, *16*, 157; b) K. I. Kim, S. Lee, X. Jin, S. J. Kim, K. Jo, J. H. Lee, *Small* **2017**, *13*, 1601926.
- [78] M. Fischler, U. Simon, H. Nir, Y. Eichen, G. A. Burley, J. Gierlich, P. M. Gramlich, T. Carell, *Small* **2007**, *3*, 1049.
- [79] K. Keren, M. Krueger, R. Gilad, G. Ben-Yoseph, U. Sivan, E. Braun, *Science* **2002**, *297*, 72.
- [80] D. R. Ranasinghe, B. R. Aryal, T. R. Westover, S. Jia, R. C. Davis, J. N. Harb, R. Schulman, A. T. Woolley, *Molecules* **2020**, *25*, 4817.
- [81] R. N. Nurdillayeva, A. B. Oshido, T. A. Bamford, O. El-Zubir, A. Houlton, J. Hedley, A. R. Pike, B. R. Horrocks, *Nanotechnology* **2018**, *29*, 135704.
- [82] F. Gao, J. Lei, H. Ju, *Anal. Chem.* **2013**, *85*, 11788.
- [83] N. Amini, M. Shamsipur, A. Maleki, *Bioelectrochem.* **2020**, *132*, 107419.
- [84] a) J. Lu, L. Yang, A. Xie, Y. Shen, *Biophys. Chem.* **2009**, *145*, 91; b) S. Kundu, K. Wang, D. Huitink, H. Liang, *Langmuir* **2009**, *25*, 10146.
- [85] L. Zhou, W. Li, Z. Chen, E. Ju, J. Ren, X. Qu, *Chemistry* **2015**, *21*, 2930.
- [86] S. M. Watson, M. A. Galindo, B. R. Horrocks, A. Houlton, *J. Am. Chem. Soc.* **2014**, *136*, 6649.
- [87] J. Liu, Y. Geng, E. Pound, S. Gyawali, J. R. Ashton, J. Hickey, A. T. Woolley, J. N. Harb, *ACS Nano* **2011**, *5*, 2240.
- [88] G. A. Burley, J. Gierlich, M. R. Mofid, H. Nir, S. Tal, Y. Eichen, T. Carell, *J. Am. Chem. Soc.* **2006**, *128*, 1398.
- [89] K. Komizo, H. Ikedo, S. Sato, S. Takenaka, *Bioconjugate Chem.* **2014**, *25*, 1547.
- [90] K. I. Kim, S. Lee, X. Jin, S. J. Kim, K. Jo, J. H. Lee, *Small* **2017**, *13*, 1601926.
- [91] Z. Chen, C. Liu, F. Cao, J. Ren, X. Qu, *Chem. Soc. Rev.* **2018**, *47*, 4017.
- [92] S. M. Watson, N. G. Wright, B. R. Horrocks, A. Houlton, *Langmuir* **2010**, *26*, 2068.
- [93] H. A. Becerril, P. Ludtke, B. M. Willardson, A. T. Woolley, *Langmuir* **2006**, *22*, 10140.
- [94] a) S. Yoon, B. Lee, J. Yun, J. G. Han, J.-S. Lee, J. H. Lee, *Nanoscale* **2017**, *9*, 7114; b) S. Yoon, C. Kim, B. Lee, J. H. Lee, *Nanoscale Adv.* **2019**, *1*, 2157.
- [95] A. O. Puchkova, P. A. Sokolov, N. A. Kasyanenko, *J. Struct. Chem.* **2011**, *52*, 1195.
- [96] M. N. Al-Hinai, R. Hassanien, N. G. Wright, A. B. Horsfall, A. Houlton, B. R. Horrocks, *Faraday Discuss.* **2013**, *164*, 71.
- [97] G. Braun, K. Inagaki, R. A. Estabrook, D. K. Wood, E. Levy, A. N. Cleland, G. F. Strouse, N. O. Reich, *Langmuir* **2005**, *21*, 10699.
- [98] A. Stern, G. Eidelstein, R. Zhuravel, G. I. Livshits, D. Rotem, A. Kotlyar, D. Porath, *Adv. Mater.* **2018**, *30*, e1800433.
- [99] S. Anantharaj, K. Sakthikumar, A. Elangovan, G. Ravi, T. Karthik, S. Kundu, *J. Colloid Interface Sci.* **2016**, *483*, 360.
- [100] S. A. K. Sakthikumar, S. R. Ede, K. Karthick, S. Kundu, *J. Mater. Chem. C* **2016**, *4*, 6309.
- [101] K. Karthick, S. Anantharaj, S. R. Ede, S. S. Sankar, S. Kumaravel, A. Karmakar, S. Kundu, *Adv. Colloid Interface Sci.* **2020**, *282*, 102205.
- [102] M. Mertig, L. C. Ciacchi, R. Seidel, W. Pompe, *Nano Lett.* **2002**, *2*, 841.
- [103] D. R. R. Basu, R. Aryal, T. R. Westover, D. G. Calvopiña, R. C. Davis, J. N. Harb, A. T. Woolley, *Nano Res.* **2020**, *13*, 1419.
- [104] A. Rotaru, S. Dutta, E. Jentsch, K. Gothelf, A. Mokhir, *Angew. Chem. Int. Ed.* **2010**, *49*, 5665.
- [105] a) S. Jayaraman, W. Tang, R. Yongsunthorn, *J. Electrochem. Soc.* **2011**, *158*, K123; b) A. O. Puchkova, P. Sokolov, Y. V. Petrov, N. A. Kasyanenko, *J. Nanopart. Res.* **2011**, *13*, 3633.

- [106] J. Ustarroz, J. A. Hammons, T. Altantzis, A. Hubin, S. Bals, H. Terry, *J. Am. Chem. Soc.* **2013**, *135*, 11550.
- [107] a) D. Xia, Z. Ku, S. C. Lee, S. R. Brueck, *Adv. Mater.* **2011**, *23*, 147; b) S. W. Yang, T. Vosch, *Anal. Chem.* **2011**, *83*, 6935.
- [108] L. Berti, A. Alessandrini, P. Facci, *J. Am. Chem. Soc.* **2005**, *127*, 11216.
- [109] L. Berti, A. Alessandrini, C. Menozzi, P. Facci, *J. Nanosci. Nanotechnol.* **2006**, *6*, 2382.
- [110] J. Samson, A. Varotto, P. C. Nahirney, A. Toschi, I. Piscopo, C. M. Drain, *ACS Nano* **2009**, *3*, 339.
- [111] S. Kundu, V. Maheshwari, R. F. Saraf, *Langmuir* **2008**, *24*, 551.
- [112] Y. Ding, G. Gu, H. L. Yang, X. H. Xia, *J. Nanosci. Nanotechnol.* **2009**, *9*, 2381.
- [113] S. Kundu, S. I. Yi, L. Ma, Y. Chen, W. Dai, A. M. Sinyukov, H. Liang, *Dalton Trans.* **2017**, *46*, 9678.
- [114] S. Kundu, H. Liang, *Colloids Surf., A* **2011**, *377*, 87.
- [115] S. Kundu, M. Jayachandran, *RSC Adv.* **2013**, *3*, 16486.
- [116] S. Kundu, H. Liang, *Adv. Mater.* **2008**, *20*, 826.
- [117] A. Henglein, *Langmuir* **1999**, *15*, 6738.
- [118] S. Eustis, M. A. El-Sayed, *J. Phys. Chem. B* **2006**, *110*, 14014.
- [119] A. A. Zinchenko, N. Chen, S. Murata, *J. Synth. Org. Chem.* **2006**, *64*, 1122.
- [120] J. Lee, H. S. Park, S. Lim, K. Jo, *Chem. Commun.* **2013**, *49*, 4740.
- [121] U. Nithyanantham, S. R. Ede, S. Kundu, *J. Mater. Chem. C* **2014**, *2*, 3782.
- [122] K. Keren, S. Berman Rotem, E. Buchstab, U. Sivan, E. Braun, *Science* **2003**, *302*, 1380.
- [123] C. T. Wirges, J. Timper, M. Fischler, A. S. Sologubenko, J. Mayer, U. Simon, T. Carell, *Angew. Chem. Int. Ed.* **2009**, *48*, 219.
- [124] J. Gierlich, G. A. Burley, P. M. Gramlich, D. M. Hammond, T. Carell, *Org. Lett.* **2006**, *8*, 3639.
- [125] J. Timper, K. Gutmiedl, C. Wirges, J. Broda, M. Noyong, J. Mayer, T. Carell, U. Simon, *Angew. Chem. Int. Ed.* **2012**, *51*, 7586.
- [126] M. Fischler, A. Sologubenko, J. Mayer, G. Clever, G. Burley, J. Gierlich, T. Carell, U. Simon, *Chem. Commun.* **2008**, *2*, 169.
- [127] J. H. Lee, D. P. Wernette, M. V. Yigit, J. Liu, Z. Wang, Y. Lu, *Angew. Chem. Int. Ed.* **2007**, *46*, 9006.
- [128] J. H. Lee, N. Y. Wong, L. H. Tan, Z. Wang, Y. Lu, *J. Am. Chem. Soc.* **2010**, *132*, 8906.
- [129] S. Roy, M. Olesiak, P. Padar, H. McCuen, M. H. Caruthers, *Org. Biomol. Chem.* **2012**, *10*, 9130.
- [130] S. Roy, M. Olesiak, S. Shang, M. H. Caruthers, *J. Am. Chem. Soc.* **2013**, *135*, 6234.
- [131] S. Ganguly, S. Paul, O. Yehezkeli, J. Cha, M. H. Caruthers, *Chem. Mater.* **2017**, *29*, 2239.
- [132] B. M. Zeglis, V. C. Pierre, J. K. Barton, *Chem. Commun.* **2007**, *44*, 4565.
- [133] K. Komizo, S. Ikedo, H. F. Sato, S. Sato, S. F. Takenaka, S. Takenaka, *Bioconjugate Chem.* **2014**, *25*, 1547.
- [134] T. Himuro, R. Araki, H. Ikedo, S. Sato, S. Takenaka, T. Yasuda, in *17th Int. Conf. Miniaturized Systems for Chemistry and Life Sciences, MicroTAS 2013*, Freiburg, Germany, Vol. 3, **2013**, p. 1466.
- [135] M. Noyong, K. Gloddek, J. Mayer, T. Weirich, U. Simon, *J. Cluster Sci.* **2007**, *18*, 193.
- [136] M. Noyong, K. Gloddek, U. Simon, *MRS Proc.* **2002**, *761*, C.9.4.1.
- [137] Y. Hashimoto, Y. Matsuo, K. Ijiro, *Chem. Lett.* **2005**, *34*, 112.
- [138] H. Mitomo, Y. Watanabe, Y. Matsuo, K. Niikura, K. Ijiro, *Chem. Asian J.* **2015**, *10*, 455.
- [139] M. Slim, N. Durisic, P. Grutter, H. F. Sleiman, *ChemBioChem* **2007**, *8*, 804.
- [140] N. Kasyanenko, Z. Qiushi, V. Bakulev, M. Osolodkov, P. Sokolov, V. Demidov, *Polymers* **2017**, *9*, 211.
- [141] L. Lombardi, G. Prenna, L. Okolicsanyi, A. Gautier, *J. Histochem. Cytochem.* **1971**, *19*, 161.
- [142] Y. Kabiri, A. Angelin, I. Ahmed, H. Mutlu, J. Bauer, C. M. Niemeyer, H. Zandbergen, C. Dekker, *ChemBioChem* **2019**, *20*, 822.
- [143] S. Lee, Y. Oh, J. Lee, S. Choe, S. Lim, H. S. Lee, K. Jo, D. C. Schwartz, *Nucleic Acids Res.* **2016**, *44*, e6.
- [144] X. L. Jin, N. D. Hapsari, S. Lee, K. Jo, *Analyst* **2020**, *145*, 4079.
- [145] U. O. Seker, H. V. Demir, *Molecules* **2011**, *16*, 1426.
- [146] a) B. Lang, N. Blot, E. Bouffartigues, M. Buckle, M. Geertz, C. O. Gualerzi, R. Mavathur, G. Muskhelishvili, C. L. Pon, S. Rimsky, S. Stella, M. M. Babu, A. Travers, *Nucleic Acids Res.* **2007**, *35*, 6330; b) R. Reeves, M. S. Nissen, *J. Biol. Chem.* **1990**, *265*, 8573; c) E. Shin, W. Kim, S. Lee, J. Bae, S. Kim, W. Ko, H. S. Seo, S. Lim, H. S. Lee, K. Jo, *Sci. Rep.* **2019**, *9*, 17197; d) T. M. Nguyen, E. Nakata, Z. Zhang, M. Saimura, H. Dinh, T. Morii, *Chem. Sci.* **2019**, *10*, 9315; e) E. Nakata, F. F. Liew, C. Uwatoko, S. Kiyonaka, Y. Mori, Y. Katsuda, M. Endo, H. Sugiyama, T. Morii, *Angew. Chem. Int. Ed.* **2012**, *51*, 2421.
- [147] J. S. Kim, C. O. Pabo, *Proc. Natl. Acad. Sci. U.S.A.* **1998**, *95*, 2812.
- [148] J. Park, S. Lee, N. Won, E. Shin, S. H. Kim, M. Y. Chun, J. Gu, G. Y. Jung, K. I. Lim, K. Jo, *Analyst* **2019**, *144*, 921.
- [149] K.-I. Kim, S. Yoon, J. Chang, S. Lee, H. H. Cho, S. H. Jeong, K. Jo, J. H. Lee, *Small* **2020**, *16*, 1905821.
- [150] Y. Ryu, Z. Jin, J.-J. Lee, S.-H. Noh, T.-H. Shin, S.-M. Jo, J. Choi, H. Park, J. Cheon, H.-S. Kim, *Angew. Chem. Int. Ed.* **2015**, *54*, 923.
- [151] H. Dai, W.-S. Choe, C. K. Thai, M. Sarikaya, B. A. Traxler, F. Baneyx, D. T. Schwartz, *J. Am. Chem. Soc.* **2005**, *127*, 15637.
- [152] R. Hall Sedlak, M. Hnilova, E. Gachelet, L. Przybyla, D. Dranow, T. Gonen, M. Sarikaya, C. Tamerler, B. Traxler, *ChemBioChem* **2010**, *11*, 2108.
- [153] P. F. Hansmann, H. Falk, U. Scheer, P. Sitte, *Eur. J. Cell Biol.* **1986**, *42*, 152.
- [154] a) M. Thiry, *Exp. Cell Res.* **1988**, *179*, 204; b) M. Thiry, D. Dombrowicz, *Biol. Cell* **1988**, *62*, 99.
- [155] M. Thiry, *Exp. Cell Res.* **1992**, *200*, 135.
- [156] a) M. Thiry, D. Ploton, M. Menager, G. Goessens, *Cell Tissue Res.* **1993**, *271*, 33; b) M. Thiry, *Microsc. Res. Tech.* **1995**, *31*, 4.
- [157] a) M. Bendayan, *Histochem. J.* **1981**, *13*, 699; b) M. Bendayan, *J. Histochem. Cytochem.* **1981**, *29*, 531; c) I. Raska, B. L. Armbruster, M. Jira, I. Hana, J. Kaslik, J. Rovinsky, K. Smetana, *Biol. Cell* **1983**, *48*, 211.
- [158] P. Trzaskoma, B. Ruszczycki, B. Lee, K. K. Pels, K. Krawczyk, G. Bokota, A. A. Szczepankiewicz, J. Aaron, A. Walczak, M. A. Sliwinska, A. Magalska, M. Kadlof, A. Wolny, Z. Parteka, S. Arabasz, M. Kiss-Arabasz, D. Plewczynski, Y. Ruan, G. M. Wilczynski, *Nat. Commun.* **2020**, *11*, 2120.
- [159] D. C. Bell, W. K. Thomas, K. M. Murtagh, C. A. Dionne, A. C. Graham, J. E. Anderson, W. R. Glover, *Microsc. Microanal.* **2012**, *18*, 1049.
- [160] A. Loukanov, C. Filipov, P. Mladenova, S. Toshev, S. Emin, *Microsc. Res. Tech.* **2016**, *79*, 280.
- [161] C. Own, A. Bleloch, W. Lerach, C. Howell, M. Hamalainen, J. Herschleb, C. Melville, J. Stark, M. Andregg, W. Andregg, *Microsc. Microanal.* **2013**, *19*, 208.



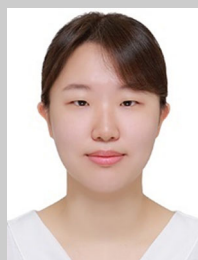
Xuelin Jin is a lecturer at Yanbian University, College of Agriculture. He obtained B.S. in chemical engineering from the Yanbian University of Science and Technology, China. He studied bioengineering at Chung-Ang University for his M.S. He graduated from the Ph.D. program at Sogang University, Department of Chemistry. Then, he moved to Yanbian University in 2021. His research interests focus on DNA–protein interactions, DNA imaging, and DNA-binding fluorescent proteins using single-molecule observation approaches.



Shrute Kannappan is a graduate student at Sungkyunkwan University (SKKU), School of Medicine, and the Research Center for Advanced Materials Technology at SKKU. She obtained her B.Tech. (Honors) in biotechnology from SASTRA Deemed to be University, India in 2020. Currently, she is doing a master's integrated Ph.D. degree program at SKKU. Her current research interest is focused on the rational design of DNA-binding peptides for DNA sequence analysis.



Natalia Diyah Hapsari is a lecturer at Sanata Dharma University. She obtained her B.Ed. and M.Ed. from Sebelas Maret University, Indonesia. She graduated from the Ph.D. program at Sogang University, Department of Chemistry. Since 2017, she has been a faculty member of the Chemistry Education Program, Department of Mathematics and Science Education at Sanata Dharma University.



Yu Jin obtained her B.S. and M.S. in chemistry from Sogang University. Her research was focused on analyzing DNA sequences using streptavidin-fluorescent proteins.



Kyeong Kyu Kim is a professor at Sungkyunkwan University School of Medicine. He obtained his B.S., M.S., and Ph.D. from Seoul National University. He worked at UC Berkeley for 3 years as a postdoc. Then, he moved to Sungkyunkwan University in 2000. His research interest is the structural and functional understanding of noncanonical DNAs in the genome, and their chemical modulation for diagnostic and therapeutic purposes.



Jung Heon Lee is an associate professor at Sungkyunkwan University (SKKU). He obtained his Ph.D. in materials science and engineering from the University of Illinois at Urbana-Champaign. After postdoctoral training at Northwestern University, he joined the School of Advanced Materials Science and Engineering at SKKU as a faculty in 2012. His research is focused on developing nanoscale materials or devices that can be applied to diverse levels of biological systems for diagnostics or therapeutics. He is also investigating strategies for exploiting the tunable properties of biomolecules such as DNA and peptides for the assembly of various nanoscale structures.



Kyubong Jo is a professor at Sogang University. He obtained his B.S. and M.S. from Seoul National University, and then spent 6 years working at the Samsung Advanced Institute of Technology. He later moved to the United States, where he obtained his Ph.D. in chemistry from the University of Wisconsin–Madison in 2006. After completing his doctoral studies, he worked as a postdoctoral researcher at the University of Illinois at Urbana-Champaign. Since 2008, he has been a faculty member in the Department of Chemistry and the Interdisciplinary Program of Integrated Biotechnology at Sogang University. Dr. Jo's research is focused on developing methods for DNA sequence analysis using high-resolution microscopic imaging techniques. Specifically, he is interested in using fluorescence and electron microscopy to visualize individual DNA molecules and developing novel methods for sequence-specific labeling and imaging of DNA. His work has the potential to improve our understanding of the structure and function of DNA at the molecular level, and to enable new advances in genomics and biotechnology.